Multi-tiered actions of *Legionella* effectors to modulate host Rab10 dynamics

Tomoko Kubori[a*], Kohei Arasaki[b], Hiromu Oide [b], Tomoe Kitao[a], and Hiroki Nagai[a,c*]

[a]Department of Microbiology, Graduate School of Medicine, Gifu University, Gifu, Gifu 501-1194, Japan
[b]School of Life Sciences, Tokyo University of Pharmacy and Life Sciences, Hachioji, Tokyo 192-0392, Japan
[c]Center for One Medicine Innovative Translational Research, Gifu University Institute for Advanced Study, Gifu, Gifu 501-1194, Japan

*Correspondence: kubori.tomoko.j0@f.gifu-u.ac.jp (T. Ku.) and nagai.hiroki.d3@f.gifu-u.ac.jp (H. N.)

Abstract

Rab GTPases are representative targets of manipulation by intracellular bacterial pathogens for hijacking membrane trafficking. *Legionella pneumophila* recruits many Rab GTPases to its vacuole and exploits their activities. Here, we found that infection-associated regulation of Rab10 dynamics involves ubiquitin signaling cascades mediated by the SidE and SidC families of *Legionella* ubiquitin ligases. Phosphoribosyl-ubiquitination of Rab10 catalyzed by the SidE ligases is crucial for its recruitment to the bacterial vacuole. SdcB, the previously uncharacterized SidC family effector, resides on the vacuole and contributes to retention of Rab10 at the late stages of infection. We further identified MavC as a negative regulator of SdcB. By the transglutaminase activity, MavC crosslinks ubiquitin to SdcB and suppresses its function, resulting in elimination of Rab10 from the vacuole. These results demonstrate that the orchestrated actions of many *L. pneumophila* effectors fine-tune the dynamics of Rab10 during infection.

Introduction

Legionella pneumophila utilizes a large arsenal of effector proteins which are delivered via its Dot/Icm type IV secretion system (T4SS) to modulate host cellular systems (Hubber and Roy, 2010; Kubori and Nagai, 2016). The functions of the effector proteins are crucial for establishing a replicative niche where *L. pneumophila* can survive and avoid host defense mechanisms in the cell (Isberg et al., 2009; Qiu and Luo, 2017). Many effector proteins are known to modulate the function of host Rab GTPases that regulates cellular membrane transport (Neunuebel and Machner, 2012; Sherwood and Roy, 2013; Spanò and Galán, 2018). Among them, effector manipulation of Rab1, a critical regulator of membrane trafficking between ER and the Golgi complex, has been extensively analyzed in *L. pneumophila* infection (Arasaki et al., 2012; Ingmundson et al., 2007; Machner and Isberg, 2006; Mukherjee et al., 2011; Müller et al., 2010; Murata et al., 2006; Neunuebel et al., 2011; Tan and Luo, 2011).

Ubiquitination regulates all aspects of eukaryotic cell physiology, and therefore is exploited by various bacterial pathogens encoding ubiquitin (Ub) ligases and deubiquitinases (DUBs) (Ashida and Sasakawa, 2017; Kitao et al., 2020; Kubori et al., 2019; Lin and Machner, 2017). Effector-mediated Ub modification of Rab1 was reported as an action of the *Legionella* E3 ligase SidC and its paralog SdcA (Horenkamp et al., 2014). Rab33b as well as Rab1, Rab6A, and Rab30 are conjugated with phosphoribosylated (PR)-Ub by the unique reaction mechanism of the SidE family of effector proteins (Qiu et al., 2016), and it was shown that recruitment of Rab33b and Rab6A to the *Legionella*-containing vacuole (LCV) relies on the PR-ubiquitination of Rab33b (Kawabata et al., 2021). A recent genome-wide screen identified host factors including Rab10 linked to intracellular replication of *L. pneumophila* (Jeng et al., 2019). It was demonstrated that Rab10 is recruited to the LCV and is ubiquitinated depending on the activity of SidC and SdcA (Jeng et al., 2019; Liu et al., 2020).

SidC and SdcA were originally identified as tethering factors that function in ER-to-LCV trafficking both having a unique phosphatidylinositol-4 phosphate (PI[4]P)-binding domain (Ragaz et al., 2008). The enzymatic activity of these proteins as Ub ligases was experimentally uncovered later (Hsu et al., 2014). The enzymatic activity was found to be encoded in the domain conserved between the two proteins, namely SidC N-terminal Ub ligase (SNL) domain (Hsu et al., 2014). SdcB (Lpg2452/LegA14) was identified as

another *L. pneumophila* Ub ligase having the SNL domain (Lin et al., 2018). However, the role of SdcB in *L. pneumophila* infection has not been examined yet.

Various *L. pneumophila* effector proteins exploit the host Ub signaling cascade (Kitao et al., 2020; Luo et al., 2021; Tomaskovic et al., 2022). They are exemplified by MavC which was shown to chemically modify the E2 enzyme UBE2N. The transglutaminase activity of MavC catalyzes a covalent linkage between Ub and UBE2N, thereby abolishing the activity of UBE2N to form polyUb chains, and mediate host NFκB signaling (Gan et al., 2019a). Encoded by the neighboring gene of *mavC*, MvcA is a paralog of MavC and exhibits similar activity to MavC as a Ub-specific deamidase (Valleau et al., 2018). However, MvcA was found to have an ability to reverse MavC-mediated Ub conjugation to UBE2N by its unique DUB activity (Gan et al., 2020). The enzymatic activities of MavC and MvcA are both inhibited by Lpg2149, an effector encoded downstream of *mvcA*, by blocking their catalytic residues (Valleau et al., 2018).

In this study, we investigated the role of *Legionella* Ub ligases in Rab10 dynamics during *L. pneumophila* infection. Including the unexpected finding that MavC is a negative regulator of SdcB, we demonstrated muti-tiered regulation by many effectors to finely modulate the localization of Rab10 to the LCV, revealing the intricate effector network that hijacks cellular processes.

Results

The SidE- and SidC-family proteins differentially contribute to ubiquitination of Rab10 in infected cells

Host Rab10 is required for optimal intracellular replication of *L. pneumophila* (Jeng et al., 2019) and therefore considered to play a significant role in LCV biogenesis or maintenance. Since *L. pneumophila* SidE family proteins, which catalyze PR-linked ubiquitination, have a wide range of substrates including Rab1 and Rab33b (Bhogaraju et al., 2016; Kalayil et al., 2018; Kotewicz et al., 2017; Qiu et al., 2016), we first examined whether the SidE family can affect Rab10 ubiquitination. Upon infection of HEK293T-FcγRII cells transiently expressing FLAG-Rab10 and HA-Ub with a wild-type *L. pneumophila* strain (Lp01) for 1 h, Rab10 was detected with a shifted band of higher molecular mass (Figure 1a upper panel). The band was shown to contain Ub by probing with an anti-HA antibody (Figure 1a lower panel), indicating that the band represents Rab10 conjugated with a single Ub molecule. The mass shift was not detected in cells

102 infected with the T4SS-deficient strain (Δ*dotA*), suggesting that Rab10 can be
103 monoubiquitinated in a T4SS-dependent manner. Infection with a Δ*sidEs* strain lacking
104 all four SidE-family proteins (SidE, SdeA, SdeB and SdeC) mostly eliminated the
105 molecular mass shift of Rab10, while infection with a strain lacking the negative
106 regulators of SidE family proteins (DupA, DupB, SidJ and SdjA (Black et al., 2019; Gan
107 et al., 2019b; Qiu et al., 2017; Shin et al., 2020; Sulpizio et al., 2019)) enhanced the
108 intensity of the band (Figure 1a). These results suggest that the SidE-family proteins can
109 conjugate PR-Ub to Rab10. The high molecular weight smears detected with anti-HA
110 antibody are thought to be polyUb chains (Figure 1a lower panel). Appearance of these
111 smears is tightly associated with the PR-Ub bands, showing that polyubiquitination of
112 Rab10 is linked with its PR-ubiquitination.
113
114 To examine if PR-Ub conjugation to Rab10 can enhance its modification with polyUb
115 chains, we infected HEK293T-FcγRII cells expressing FLAG-Rab10 and HA-Ub with
116 the Δ*sidEs* strain complemented with a plasmid expressing wild-type or a catalytic mutant
117 of SdeA ($SdeA_{EE/AA}$), a representative SidE-family protein (Figure 1b). We detected a
118 strongly enhanced polyUb smear whose appearance depends on the mono-ADP
119 ribosyltransferase activity of SdeA. The intensity of the monoubiquitination band was
120 correlated with that of the polyUb smears (Figure 1b middle panel). When the C-terminal
121 GG motif of Ub was replaced with AA (Ub_{AA}), the polyUb smear drastically diminished,
122 and accumulation of monoUb-conjugated Rab10 was observed instead. This indicates
123 that the polyUb chains on Rab10 were formed via the Ub C-terminus by the canonical
124 ubiquitination reaction. This also shows that the observed monoUb-conjugation to Rab10
125 does not require the Ub C-terminus, which is consistent with the formation of bridge
126 between Arg42 of Ub and substrate catalyzed by the SidE effectors (Bhogaraju et al.,
127 2016; Kotewicz et al., 2017; Qiu et al., 2016). These results strongly support that Rab10
128 is subjected to SdeA-mediated PR-ubiquitination and that this modification may provide
129 a platform of conjugation of polyUb chains to Rab10, which is expected to be mediated
130 by other Ub ligases.
131
132 Since it was reported that *L. pneumophila* effectors SidC and its paralog SdcA induce
133 Rab10 ubiquitination (Jeng et al., 2019; Liu et al., 2020), we investigated how these E3
134 ligases contribute towards ubiquitination of Rab10 in our system (Figure 1c). Infection of
135 cells with a Δ*sidC*Δ*sdcA* strain as well as with a strain lacking all the SidC family proteins
136 (Δ*sidC*Δ*sdcA*Δ*sdcB*) still caused both mono- and polyubiquitination of Rab10 but with
137 reduced levels. On the contrary, infection with the Δ*sidEs* strain eliminated both

modifications. These results support that SidE-family proteins primarily contribute towards ubiquitination of Rab10, and that SidC-family proteins partly contribute towards polyubiquitination of Rab10 directly or indirectly in conditions where Rab10 is modified with PR-Ub. We also found that substitution of three residues on Rab10 (Lys102, Lys136, and Lys154) that were previously suggested to be potential ubiquitination sites (Jeng et al., 2019) to Ala (Rab10KKK) did not abolish polyubiquitination of Rab10 (Figure 1-figure supplement 1a), implying that ubiquitination sites can be present in the other residues. This raises the possibility that canonical Ub chains can be formed partly on PR-Ub conjugated to Rab10. The polyubiquitination of Rab10 was significantly observed until 7 h after infection, although the level was slightly reduced (Figure-figure supplement 1b).

Rab10 recruitment to the LCV is differentially regulated by SidE- and SidC-family proteins

Earlier studies demonstrated that Rab10 ubiquitination is highly correlated with its localization to the LCV (Jeng et al., 2019; Liu et al., 2020). We therefore examined if the SidE family regulates Rab10 recruitment to the LCV using HeLa-FcγRII cells transiently expressing RFP-Rab10 (Figure 2a and b). Infection with the Δ*sidEs* strain drastically reduced the level of Rab10-positive LCVs at all time points examined (Figure 2b). As reported for Rab33b (Kawabata et al., 2021), PR-ubiquitination is thought to be required for Rab10 to localize to the LCV. The Δ*sidC*Δ*sdcA* LCV also exhibited a reduced the level of Rab10 localization at 1 h after infection (Figure 2b left panel). However, the level of Rab10 recruitment to the Δ*sidC*Δ*sdcA* LCV recovered at 4 h after infection, while that to the Δ*sidC*Δ*sdcA*Δ*sdcB* LCV did not recover even as late as 7 h (Figure 2b middle and right panels). This result suggests that SdcB can contribute towards retention of Rab10 on the LCV at late stages of infection.

SdcB associates with the LCV and plays a major role in Ub recruitment to the LCV at late stages of infection

The Ub accumulation on the LCV has been thought to be mediated largely by SidC and SdcA (Horenkamp et al., 2014; Luo et al., 2015). We therefore examined the possible role of SdcB in Ub recruitment to the LCV at distinct time points after infection (Figure 3). To mask the effect of SidC and SdcA, we used a Δ*sidC*Δ*sdcA*Δ*sdcB* strain complemented with wild-type or catalytic mutant (C57A) of SdcB expressed from a plasmid. When HeLa-FcγRII cells were infected with these strains for 1 h, SdcB was detected around the LCV (Figure 3a and b). The level of wild-type SdcB-positive LCVs was relatively lower

compared with that of the $SdcB_{C57A}$-positive LCVs, probably due to its catalytic cycling. The expression of wild-type SdcB led to recruitment of Ub to the vacuole even without SidC and SdcA, while expression of $SdcB_{C57A}$ did not (Figure 3b). This result indicates that SdcB has a catalytic activity to conjugate Ub to substrates on the LCV. At 7 h after infection, the level of the SdcB-positive LCVs was elevated to about 70 % regardless of its catalytic activity (Figure 3c and d). At this time point, the level of the Ub-positive LCVs was also raised to about 60 %, but only when SdcB was catalytically active. These results demonstrate that SdcB can play a substantial role to conjugate Ub to substrates on the LCV at late stages of infection.

The catalytic activity of SdcB enhances retention of Rab10 on the LCV

As Rab10 is one of the plausible substrates located on the LCV, we assessed its ubiquitination upon infection with the *L. pneumophila* strains for comparison between its GTP-bound active (QL) and GDP-bound inactive (TN) conformations (Figure 4a). A substantial amount of ubiquitinated Rab10QL, but not Rab10TN, was detected upon infection with the wild-type strain (Figure 4a; Figure 4-figure supplement 1). We found that ubiquitination of Rab10TN detected with HA-probing (HA-Ub) was apparently indirect and not infection-induced, as FLAG-probing (FLAG-Rab10) mostly eliminated the high molecular weight smears on Rab10TN (Figure 4-figure supplement 1). Polyubiquitinated Rab10QL was reduced by infection with the Δ*sidC*Δ*sdcA*Δ*sdcB* strain, while both mono- and polyubiquitination of Rab10QL was mostly blocked by infection with the Δ*sidEs* strain. Localization of active Rab10 (Rab10QL) on the LCVs was apparently correlated with the level of its polyubiquitination (Figure 4b, Figure 4-figure supplement 2). The finding that the active form of Rab10 is preferentially targeted and spatially regulated by the action of SidE- and SidC-family ligases prompted us to examine the effect of SdcB activity on ubiquitination of this specific form of Rab10. Bacterially expressed SdcB, but not its catalytic mutant, significantly enhanced the level of polyubiquitination of Rab10QL at 7 h after infection (Figure 4c). To examine the relationship between the catalytic activity of SdcB and the LCV localization of Rab10, we assessed the level of Rab10-positive LCVs on which SdcB localized. At 7 h post infection, Rab10 localization was readily detected on Δ*sidC*Δ*sdcA*Δ*sdcB* LCVs containing wild-type SdcB, but not the inactive $SdcB_{C57A}$ mutant (Figure 4d). The level of Rab10-positive LCVs was significantly higher with expression of wild-type SdcB than that of the catalytic mutant (Figure 4e), suggesting that the Ub ligation activity of SdcB supports retention of Rab10 on the LCV until late stages of infection.

210 **MavC modifies SdcB when ectopically expressed in cells**
211 A potential relationship between SdcB and MavC as an effector/metaeffector pair was
212 suggested by a recent systematic analysis utilizing yeast genetics (Urbanus et al., 2016).
213 We therefore examined whether expression of MavC can affect the activity profile of
214 SdcB in cells. When ectopically expressed in HEK293T-FcγRII cells, 3xFLAG-tagged
215 SdcB could not be detected (Figure 5a top panel, most left lane). However, we found that
216 coexpression of GFP-tagged MavC, but not of its catalytic mutant ($MavC_{C74A}$), recovered
217 the detection of SdcB (Figure 5a top panel). As SdcB was resolved as a doublet in the
218 immunoblot, we suspected that SdcB may be chemically modified by MavC and that the
219 modification may result in enhanced detection of this protein. We therefore probed with
220 an anti-HA antibody to detect possible Ub conjugation. The upper band was stained with
221 anti-HA antibody, showing that Ub was conjugated to SdcB presumably by the known
222 Ub conjugation ability of MavC (Gan et al., 2019a) (Figure 5a middle panel). We also
223 found that the disappearance of the SdcB bands correlated with the appearance of the high
224 molecular weight smears when probed with anti-HA antibody (Figure 5a middle panel).
225 This suggests that the disappearance of the SdcB band can be caused by auto-
226 ubiquitination, as SdcB has an ability to catalyze auto-ubiquitination with a diverse
227 repertoire of E2 enzymes (Figure 5-figure supplement 1) consistently with a previous
228 report (Lin et al., 2018). A proteasome inhibitor MG132 treatment of the cells did not
229 rescue the disappearance of the SdcB bands, suggesting that auto-ubiquitinated SdcB was
230 not subjected to proteasomal degradation (Figure 5-figure supplement 2a), but the auto-
231 ubiquitination rather caused its apparent loss by the band distribution on the gel. The
232 catalytic activity-dependent reduction of apparent SdcB level was also detected in
233 infected cells (Figure 4c, bottom panel). The transglutaminase activity of MavC is likely
234 required for conjugation of Ub to SdcB, as the catalytic mutant of MavC ($MavC_{C74A}$)
235 failed to modify SdcB (Figure 5a). We also found that unmodified SdcB was readily
236 detected when the SdcB C57 active site was mutated regardless of the presence of MavC
237 (Figure 5b top panel), consistent with the disappearance of the band was linked to the
238 auto-ubiquitination ability. Interestingly, the MavC-mediated Ub conjugation to $SdcB_{C57A}$
239 was not readily detected (Figure 5b). This indicates that the catalytic residue C57 of SdcB
240 is crucial in being modified by MavC. As suggested by the reduction of the high molecular
241 weight smears (Figure 5a), it is plausible that MavC suppresses the E3 ligase activity of
242 SdcB by the unique chemical modification.
243
244 **The transglutaminase activity of MavC mediates Ub conjugation to SdcB and to**
245 **SdcA**

To confirm the direct involvement of MavC in the unique Ub modification of SdcB, we reconstructed an *in vitro* reaction using purified proteins. In the presence of MavC, but not of its paralog MvcA, the mass shift of SdcB was readily detected (Figure 5c top panel). The immunoblotting showed that the band contains Ub (Fig. 5C middle panel). The presence of wild-type MavC, but not its catalytic mutant, also reduced SdcB auto-ubiquitination *in vitro* (Figure 5-figure supplement 2b). Since SidC, SdcA and SdcB are paralogs to each other, we examined if SidC and/or SdcA are also subject to MavC-mediated Ub conjugation. Triple-FLAG-tagged SidC or SdcA were transiently expressed together with GFP-MavC and HA-Ub in HEK293T-FcγRII cells, and the 3xFLAG-tagged proteins were immunoprecipitated (Figure 5d). These results clearly demonstrated that Ub was conjugated to SdcA but not to SidC by the catalytic activity of MavC, and that this modification occurred only to SdcA in the catalytically active form.

We then analyzed the MavC-mediated Ub-conjugation to SdcB using derivatives of Ub (Figure 5e and f). The use of Ub having no Lys residues (HA-Ub $_{\text{No K}}$) resulted in an enhanced level of Ub-conjugation to SdcB mediated by functional MavC (Figure 5e middle panel). Surprisingly, HA-Ub$_{AA}$ did not conjugate to SdcB, indicating that the C-terminal Gly-Gly residues are essential for MavC-mediated Ub conjugation to SdcB (Figure 5f second panel). The shifted band detected by FLAG probing represents conjugation of cellular intrinsic Ub (Figure 5f top panel) as probed by Ub antibody (Figure 5f third panel).

Transglutaminase activity of MavC is known to target Gln40 of Ub to catalyze the intramolecular crosslinking (Gan et al., 2019a; Guan et al., 2020; Puvar et al., 2020). We investigated whether the same residue of Ub is crosslinked to SdcB by the activity of MavC using mass spectrometric (MS) analysis. We found that a covalent bond was formed between Gln41 of Ub and Lys518 of SdcB (Figure 6a). Crosslinking between Gln31 of Ub and Lys891 of SdcB was also detected (Figure 6-figure supplement 1). To confirm the results, we replaced Ub residues Gln41 and Gln31 with Glu (Ub $_{\text{Q41E}}$, Ub $_{\text{Q31E}}$, and Ub $_{\text{Q31E Q41E}}$) and conducted the Ub-conjugation assay by transient expression in HEK293T-FcγRII cells. Consistent with the result from the MS analysis, Ub $_{\text{Q41E}}$, but not Ub $_{\text{Q40E}}$, failed to be conjugated to SdcB, showing that Gln41 is crucial for MavC-mediated crosslinking with SdcB (Figure 6b middle panel). Ub $_{\text{Q31E}}$ also reduced the level of modified SdcB, and Ub $_{\text{Q31E Q41E}}$ completely abolished the crosslinking to SdcB. The presence of modified SdcB bands when probed with anti-FLAG antibody is thought to be caused by conjugation with intrinsic Ub in cells (Figure 6b top panel). Contrarily,

282 replacement of Lys518 and Lys891 of SdcB to Arg (SdcB $_{K518R}$, SdcB $_{K891R}$, and SdcB
283 $_{K518R\ K891R}$), which have no apparent effect on Rab10 ubiquitination (Figure 6-figure
284 supplement 2), showed lesser impact on abolishing the reactivity (Figure 6c), suggesting
285 that additional residues of SdcB can be subjected to MavC-dependent Ub conjugation.
286 Taken together, we currently hypothesize that association of the C-terminal Gly of Ub to
287 the catalytic pocket of SdcA or SdcB (C44 or C57, respectively) positions these molecules
288 in proper orientation for intramolecular crosslinking mediated by the transglutaminase
289 activity of MavC.
290
291 **Catalytic activity of MavC can impact Rab10 localization to the LCV**
292 We then examined the role of MavC in the LCV localization of Rab10. By
293 immunofluorescent microscopy, we monitored the level of RFP-tagged Rab10 on SdcB-
294 positive LCVs when MavC or its catalytic mutant were expressed in HeLa-FcγRII cells
295 (Figure 7a). At 4 h after infection with *L. pneumophila* strains expressing 3xFLAG-SdcB,
296 the level of Rab10-positive LCVs was significantly higher in the cells expressing the
297 catalytic mutant of MavC compared with those expressing wild-type MavC (Figure 7a
298 and b). That Rab10 localization was reduced coincident with MavC-dependent inhibition
299 of SdcB further supports the contribution of SdcB activity towards retention of Rab10 on
300 the LCV. We then wondered whether bacterially delivered MavC can contribute to the
301 elimination of Rab10 from the vacuole. As the levels of the Rab10-positive LCVs were
302 not significantly altered up to 7 h after infection with the wild-type *L. pneumophila* strain
303 (Figure 2b), we examined Rab10 localization at a later time point after infection (Figure
304 7c, Figure 7-figure supplement 1). At 9 h after infection with the wild-type strain, the
305 level of Rab10-positive LCVs was reduced to about 20% of the total LCVs (compare with
306 that of 1 to 7 h infection (~40%) (Figure 2b). However, the level got significantly higher
307 in the cells infected with a Δ*mavC*Δ*mvcA* strain. Contrary, when the cells were infected
308 with a strain lacking Lpg2149 which inhibits the activity of MavC and MvcA, the level
309 declined. These results support that MavC suppresses the activity of SdcB in infection
310 conditions and thereby downregulates Rab10 localization to the LCV at later stages of
311 infection. Taken together, we found that Rab10 localization is finely regulated during
312 infection; the interplay of bacterial enzymes leads to sustained association of Rab10 with
313 the LCV and eventually dissociates it from the LCV presumably in accordance with the
314 process of the LCV biogenesis (Figure 7d).
315
316 **Discussion**

317 Following the finding that subversion of Rab1 function is critical for *L. pneumophila* to
318 create the replicative vacuole (Kagan et al., 2004), remarkable numbers of studies have
319 revealed the molecular mechanisms of how *L. pneumophila* T4SS effectors modulate the
320 localization and enzymatic activity of Rab1 (Qiu and Luo, 2017). The importance of
321 Rab10 and its chaperone *RABIF* for intracellular replication of *L. pneumophila* has
322 recently emerged (Jeng et al., 2019). However, little is known about how *L. pneumophila*
323 manipulates the activity of Rab10.
324
325 We found that the SidE-family effectors mediate noncanonical ubiquitination of Rab10.
326 Apparently, this modification precedes and is prerequisite for subsequent
327 polyubiquitination of Rab10 (Figure 1), which is linked to its localization to the LCV
328 (Figure 2). Polyubiquitination of Rab10 was enhanced in a manner depending on the
329 catalytic activities of the SidC-family proteins (Figure 1, Figure 4a and c) consistent with
330 previous reports (Jeng et al., 2019; Liu et al., 2020). As ectopic expression of SdeA in
331 HEK293T-FcγRII cells led to monoubiquitination of Rab10 (Figure 7-figure supplement
332 2), it is plausible that PR-Ub conjugation to Rab10 is directly catalyzed by the SidE-
333 family ligases. However, the SdcB-mediated polyubiquitination of Rab10 was not readily
334 detected even in the presence of SdeA lacking its DUB domain (Figure 7-figure
335 supplement 2). This result prompted us to consider that polyubiquitination of Rab10 by
336 the SidC family ligases can occur only in a specific circumstance, i.e. on the LCV. It is
337 also possible that Rab10 can be partly catalyzed by canonical E3 ligases in host cells
338 and/or other *L. pneumophila* effector proteins. The Ub ligase activity of SdcB strongly
339 induced accumulation of Ub on the LCV (Figure 3), showing that Rab10 may not be an
340 only substrate of SdcB. The PR-Ub modification of Rab10 and ubiquitination of unknown
341 LCV-associated substrates of the SidC family may provide the platform for the further
342 modification of Rab10.
343
344 Involvement of MavC for regulation of the SidC-family ligases was unexpectedly
345 identified in our analyses. This finding has added another layer of complexity to effector-
346 mediated regulation of Rab10. It was previously demonstrated that MavC can catalyze
347 covalent linkage between Q40 of Ub with a Lys residue of UBE2N (Gan et al., 2019a).
348 Our result showing that Q41 of Ub is crosslinked with SdcB gives a new insight into the
349 molecular mechanism of how MavC catalyzes Ub conjugation to specific substrates. In
350 addition, both the C-terminal Gly of Ub (Figure 5f) and the catalytic Cys of SdcB (C57A)
351 (Figure 5b) were essential for crosslinking. This strongly suggests that the ability of SdcB
352 as a Ub ligase to position a Ub molecule into its active site is a requirement for MavC to

form the covalent bond between Ub and SdcB. This model is reminiscent of the reaction scheme described for how MavC mediates Ub conjugation to UBE2N, in which the initial capturing of Ub by the E2 activity of UBE2N allows enhanced activity by MavC (Puvar et al., 2020). We investigated SdcB in terms of the MavC-mediated regulation in this study and found that suppression of its activity can be beneficial for release of Rab10 at the maturation stage of LCV biogenesis (Figure 7d). However, MavC may have multiple targets including SdcA (Figure 5d) which can be involved in the early stage of infection. How MavC regulates the entire process of the vacuolar modification needs to be addressed in future studies.

In contrast to the PI[4]P-binding domain present in SidC and SdcA, SdcB has an ankyrin repeat (ANK) domain at its C-terminus. As ANK domains are generally known to mediate protein-protein interactions, we speculate that SdcB targets substrates distinct from those of SidC and SdcA. The lipid-binding ability of SidC and SdcA implicates their substrate specificity; their substrates are on or associated with the LCV in the specific stages of vacuole remodeling (Vormittag et al., 2023). We, therefore, speculate that SdcB can target substrate(s) present on the LCV in maturation stages different from ones when SidC and SdcA can work in. In spite of our extensive efforts, we have not succeeded to identify cellular targets with which the ANK domain of SdcB interacts. It would be a future perspective to understand the exact biological role of SdcB as a Ub ligase in *L. pneumophila* infection by identifying its enzymatic substrates.

We found that *L. pneumophila* has a multi-tiered regulatory mechanism to manipulate Ub signaling cascades in which SidC- and SidE-family Ub ligases are involved, even though the exact molecular mechanism how Ub modification of Rab10 results in regulation of its LCV residency would be an open question. MavC was found to contribute to fine-tuning the regulation via its unique Ub-conjugation activity toward SdcB. These regulations are reflected in many aspects of the LCV biogenesis and maturation which are thought to be largely controlled by Ub signaling. The regulatory cascade of Rab10 GTPase, whose function is crucial for ER recruitment to the LCV, became apparent in this study. Most likely, similar regulatory cascades exist for many LCV-associated proteins.

Materials and methods

Bacterial strains and growth conditions

388 The *L. pneumophila* and *Escherichia coli* strains used in this study are listed in Key
389 resource table. Deletion strains were constructed by allelic exchange, as described
390 previously (Zuckman et al., 1999). The *L. pneumophila* strains were grown at 37°C in
391 liquid N-(2-acetamido)-2-aminoethanesulfonic acid (ACES; Sigma)-buffered yeast
392 extract (AYE) media or on charcoal-yeast extract (CYE) plates (Feeley et al., 1979) with
393 or without appropriate antibiotics (100 µg /mL streptomycin, 10 µg/mL chloramphenicol,
394 and 10 µg/mL kanamycin), as described previously (Berger et al., 1994). The *E. coli*
395 strains (DH5α, DH5αλpir, and BL21[DE3]) were grown at 37°C in standard media.
396
397 **Cell culture**
398 HeLa-FcγRII cells (Arasaki et al., 2017) were grown in Minimum Essential Medium α
399 (MEMα; Gibco) supplemented with 10% fetal bovine serum (FBS; Sigma). HEK293T-
400 FcγRII cells (Arasaki and Roy, 2010) were grown in Dulbecco's Modified Eagle
401 Medium (DMEM; Gibco) supplemented with 10% FBS. All cells were incubated at
402 37ºC under 5% CO_2 condition.
403
404 **Plasmid construction**
405 Plasmids used in this study are listed in Appendix 1-table 1. All cloning was conducted
406 by PCR-amplification of the desired genes using primers listed in Appendix 2-table 2
407 from genomic DNA of *L. pneumophila* or from plasmids listed in Appendix 2-table 1
408 followed by ligation with the vectors unless otherwise noted below. Site-directed
409 mutagenesis was carried out using a QuickChange II site-directed mutagenesis Kit
410 (Agilent) according to the manufacture's recommendation. For construction of pET15b-
411 His-*sdeA*$_{\Delta DUB}$, the entire region of pET15b-His-*sdeA* except for the region encoding 1-
412 199 aa of SdeA was amplified with primers 2649/2712 and then the fragment was self-
413 ligated with a Gibson assembly kit (New England Biolabs). For construction of pmGFP-
414 *sdeA*$_{\Delta DUB}$, the entire region of pmGFP-*sdeA* except for the region encoding 1-199 aa of
415 SdeA was amplified with primers 2714/2715 and then the fragment was self-ligated with
416 a Gibson assembly kit. For construction of pMMB-3xMyc-*sdeA*, the coding region of
417 *sdeA* was amplified using primers 2658/2659 from genomic DNA of Lp01, then the
418 fragment was ligated with a linearized vector generated by PCR using 2341/2681 based
419 on pMMB-PicmR-3xFLAG.
420
421 **Protein purification**
422 *E. coli* cells overproducing MavC, MvcA or SdcB with a hexa-histidine tag were collected
423 by centrifugation and resuspended with 50 mM Tris-HCl pH 7.5, 5 mM EDTA containing

424 SigmaFast Protease Inhibitor Cocktail (Sigma). Cells were disrupted, centrifuged (30,000
425 × *g*, 20 min), and the soluble fraction was loaded on a HiPrep Q FF column (Cytiva). His-
426 tagged MacV or MvcA was eluted by a 0-500 mM gradient of NaCl in 20 mM Tris-HCl
427 pH7.5, 10 mM 2-mercaptoethanol and was loaded on a HisTrap HP column (Cytiva). His-
428 tagged protein was eluted by a 40-500 mM gradient of imidazole in 20 mM Tris-HCl pH
429 7.5, 200 mM NaCl, 10 mM 2-mercaptoethanol. Peak fractions were pooled and loaded
430 onto a HiLoad Superdex 200 gel filtration column (Cytiva). Purified protein was eluted
431 in 20 mM Tris-HCl pH 7.5, 200 mM NaCl, 1mM dithiothreitol and concentrated using a
432 Vivaspin 20 concentrator (Sartorius).
433
434 **Ub ligation assay**
435 The *in vitro* ubiquitination assay in the substrate-free system was conducted as described
436 before (Kubori et al., 2018) with minor modifications. Briefly, reaction mixtures (12.5 µl)
437 containing 5 µg of recombinant human Ub (Boston Biochem), 80 nM recombinant human
438 E1 (Boston Biochem), 400 nM recombinant human E2 enzymes (Boston Biochem) and
439 400 nM purified E3 ligases in 50 mM Tris-Cl (pH 7.5), 2 mM $MgCl_2$, 120 mM NaCl, 2
440 mM ATP and 1 mM DTT were incubated for 2 h at 30°C. The reaction was stopped by
441 adding 12.5 µl of 2xSDS sample buffer and boiling.
442
443 **Transglutaminase assay**
444 The *in vitro* transglutaminase assay was conducted using the same buffer for the Ub
445 ligation assay (omitting ATP). Reaction mixtures (12.5 µl) containing 5 µg of Ub, 400 nM
446 purified His-SdcB and 800 nM purified MavC were incubated for 1 h at 37°C. The
447 reaction was stopped by adding 12.5 µl of 2xSDS sample buffer and boiling.
448
449 **Transfection and infection**
450 HEK293T-FcγRII cells were seeded in poly-L-lysine (Sigma)-coated 6-well tissue culture
451 plates at 6×10^5 cells/well 24 h before transfection or infection. Transfection was
452 performed using Lipofectamine2000 (Invitrogen) for 24 h according to the
453 manufacturer's recommendation. HeLa-FcγRII cells were seeded on coverslips in 24-well
454 tissue culture plates at 4×10^4 cells/well 24 h before transfection or infection. Transfection
455 was performed using Polyethylenimine (PEI) for 24 hr. For infection, *L. pneumophila*
456 was harvested from a 2-days heavy patch grown on CYE plates with or without
457 appropriate antibiotics and 1 mM IPTG, and then it was resuspended in sterilized distilled
458 water. The bacteria were opsonized with anti-*Legionella* antibody (1:3,000 dilution)
459 before infection. After adding the bacteria to the cells, the plates were centrifuged at 200

460 × g to precipitate bacteria onto the layer of cells and were immediately warmed in a 37°C
461 water-bath by floating for 5 min and then placed in a CO_2 incubator at 37°C. At 1 h after
462 infection, the infected cells were washed three times with prewarmed Dulbecco's
463 Phosphate Buffered Saline (DPBS; Sigma) and refreshed with prewarmed media to
464 remove the extracellular bacteria, and incubation was resumed at 37°C in a CO_2 incubator.
465

466 **Immunoprecipitation**

467 The transfected or infected cells were washed with DPBS three times and lysed with Lysis
468 buffer (20 mM Tris-HCl, pH 7.5, 150 mM NaCl, 1 mM EDTA, 1% NonidentP40)
469 containing protease inhibitors (cOmplete; Roche), 1 mM phenylmethylsulfonyl
470 fluoride (PMSF; Nacarai), 10 mM N-Ethylmaleimide (NEM, Sigma) as a DUB inhibitor
471 and 10 μM MG132 (Calbiochem) as a proteasome inhibitor. After removal of cell debris
472 with centrifugation, cell lysates were incubated with FLAG M2 magnetic beads (Sigma),
473 RFP-Trap magnetic beads (chromotek) or Myc-Trap magnetic beads (chromotek) for 2 h
474 to overnight at 4°C. The beads were washed five times with wash buffer (20 mM Tris-
475 HCl, pH 7.5, 150 mM NaCl, 1mM EDTA, 0.1% TritonX-100), and the bead-bound
476 proteins were eluted by boiling in SDS sample buffer.
477

478 **Immunofluorescent microscopy**

479 HeLa-FcγRII cells on coverslips were fixed with 4% paraformaldehyde /DPBS for 20
480 min at room temperature and washed with DPBS three times. After permeabilization and
481 blocking with 0.2 % Triton X-100 and 2 % goat serum in DPBS for 20 min, the coverslips
482 were incubated with the primary antibodies indicated in the figure legends for 90 min.
483 After washing with DPBS three times, the coverslips were incubated with the fluorescent
484 secondary antibodies with DAPI for 40 min. After washing with DPBS three times, the
485 coverslips were mounted on glass slides using ProLong Diamond antifade mounting
486 medium (Thermo Fisher). Images were collected using an inverted microscope (TE2000-
487 U; Nikon) equipped with a digital ORCA-ERA camera (Hamamatsu).
488

489 **LC-MS/MS analysis**

490 Protein bands corresponding to MavC-mediated modification of 3xFLAG-SdcB were
491 excised from SDS-PAGE and digested with trypsin. Mass spectrometry experiments were
492 performed at the Research Institute for Microbial Diseases (RIMD). The proteins were
493 reduced with 10 mM DTT, followed by alkylation with 55 mM iodoacetamide, digested
494 by treatment with trypsin (Promega) and purified with a C18 tip (AMR, Tokyo, Japan).
495 The resultant peptides were subjected to nanocapillary reversed-phase LC-MS/MS

analysis using a C18 column (12 cm x 75 um, 1.9µm, Nikkyo technos, Tokyo, Japan) on a nanoLC system (Bruker Daltoniks, Bremen, Germany) connected to a timsTOF Pro mass spectrometer (Bruker Daltoniks) and a modified nano-electrospray ion source (CaptiveSpray; Bruker Daltoniks). The mobile phase consisted of water containing 0.1% formic acid (solvent A) and acetonitrile containing 0.1% formic acid (solvent B). Linear gradient elution was carried out from 2% to 35% solvent B for 20 min at a flow rate of 250 nL/min. The ion spray voltage was set at 1.6 kV in the positive ion mode. Ions were collected in the trapped ion mobility spectrometry (TIMS) device over 100 ms and MS and MS/MS data were acquired over an m/z range of 100–2,000. During the collection of MS/MS data, the TIMS cycle was adjusted to 0.53 s and included 1 MS plus 4 parallel accumulation serial fragmentation (PASEF)-MS/MS scans, each containing on average 12 MS/MS spectra (>100 Hz) (Meier et al., 2018, 2015) and nitrogen gas was used as collision gas.

The resulting data was processed using DataAnalysis version 5.2 (Bruker Daltoniks), resulting peak files (mgf format) were subjected to MASCOT version 2.7.0 (Matrix Science, London, UK) against the Swissprot_database(568,744 sequences; 205,548,017 residues) taxonomy limited homo sapiens (20,305 sequences), HA-Ub (1 sequences; 92 residues) and 3xFLAG-lpg2452 database (1 sequences; 950 residues), and searched with the following settings: The mass tolerance for precursor ions was ±15 ppm; The mass tolerance for fragment ions was ±0.05 Da; enzyme, Trypsin; max. missed cleavages, 4; fixed modification: carbamidomethylation on cysteine; variable modifications: oxidation of methionine, N-terminal Gln to pyro-Glu. The threshold score/expectation value for accepting individual spectra was $p < 0.05$. User defined Crosslinker setting is cross-linker: Ubiq01 (mass modification: -17.026549 Da, deamination). The cross-link reactions were assumed to connect Lysine or Glutamine. It does not pair with K and K, or Q and Q. It links only 3xFLAG-lpg2452 between HA-Ub.

Acknowledgements

We thank Tetsuya Honda, Masanari Nishikawa, Tenne Ichikawa, and Seryeong Du for their technical assistance. LC/MS-MS analysis was conducted by Akinori Ninomiya (Core Instrumentation Facility, Research Institute for Microbial Diseases, Osaka University, Japan). The 3xHA-Ub and 3xHA-Ub-AA expressing plasmids were kind gifts from Jiazhang Qiu (College of Veterinary Medicine, Jilin University, China). The HA-Ub expressing plasmid is a kind gift from Michinaga Ogawa (National Institute of Infectious

532 Diseases, Japan). We thank Jonathan N. Pruneda (Department of Molecular Microbiology
533 & Immunology, Oregon Health & Science University, USA) for providing a critical
534 review of the manuscript. This study was supported by Takeda Science Foundation (to T.
535 Ku.), MEXT/JSPS KAKENHI grants 22H02867 and 19H03469 (to T. Ku.), 20H05772
536 (to K. A.), 20K07477 (to T. Ki.), and 19H03470 (to H. N.).
537

538 **Author contributions**

539 Conceptualization, T. Ku.; Methodology, T. Ku., T. Ki., and K. A.; Investigation, T. Ku.,
540 K. A., H. O. and H. N.; Writing- Original Draft, T. Ku.; Writing-Review & Editing, T. Ku,
541 H. N., and K. A.; Funding Acquisition, T. Ku., K. A., T. Ki, and H. N. Supervision, T. Ku.
542 and H. N.
543

544 **Declaration of interests**

545 The authors declare no competing interests.
546

547 **Figure legends**
548

549 **Figure 1. The SidE- and SidC-family proteins differentially contribute towards**
550 **ubiquitination of Rab10.**

551 HEK293T-FcγRII cells transiently expressing 3xFLAG-Rab10 and HA-Ub were infected
552 with the indicated *L. pneumophila* strains for 1 h at an MOI of 20. Rab10 was isolated
553 from cell lysate by immunoprecipitation using anti-FLAG magnetic beads and was
554 probed with anti-FLAG and with anti-HA antibodies. Triple-HA-Ub (3xHA-Ub) or Ub in
555 which the C-terminal GG were replaced with AA (3xHA-Ub_{AA}) was expressed instead of
556 HA-Ub in (b). Bacterial lysates were probed with anti-Myc antibody in (b).

557 **Figure 2. The SidE- and SidC-family proteins differentially contribute towards**
558 **recruitment of Rab10 to the LCV.**

559 HeLa-FcγRII cells transiently expressing RFP-Rab10 were infected with the indicated *L.*
560 *pneumophila* strains at an MOI of 5 for 4 h (a) and for the indicated time (b). (a)
561 Representative images of infected cells. Fixed cells were stained for *L. pneumophila*
562 (green) and DNA (blue) and visualized with RFP-Rab10 (red). Magnified images in the
563 white squares are shown in merged and in each channel. Arrows indicate the Rab10-
564 positive LCVs. Scale bars, 10 μm. (b) Quantitation of Rab10-positive LCVs (%).
565 Infections were performed in triplicate and each value represents scoring from 200 LCVs.
566 Significance was determined using Student's t-test.
567

568 **Figure 3. SdcB associates with the LCV and plays a major role in Ub recruitment to**
569 **the LCV at late stages of infection.**
570 HeLa-FcγRII cells were infected with the indicated *L. pneumophila* strains at an MOI of
571 2 for 1 h (a, b) and for 7 h (c, d). (a, c) Representative images of infected cells. Fixed cells
572 were stained for FLAG-SdcB or Ub (green), *L. pneumophila* (red) and DNA (blue).
573 Magnified images in the white squares are shown in the lower panels. Scale bars, 10 μm.
574 (b, d) Quantitation of SdcB-positive (left) and of Ub-positive (right) LCVs (%). Infections
575 were performed in triplicate and each value represents scoring from 200 LCVs.
576 Significance was determined using Student's t-test.
577
578 **Figure 4. The catalytic activity of SdcB enhances retention of Rab10 on the LCV.**
579 (a) HEK293T-FcγRII cells transiently expressing 3xFLAG-Rab10 $_{Q68L}$ (QL) or Rab10
580 $_{T23N}$ (TN) with HA-Ub were infected with the indicated *L. pneumophila* strains for 1 h at
581 an MOI of 50. Rab10 was isolated from cell lysate by immunoprecipitation using anti-
582 FLAG magnetic beads and was probed with anti-FLAG antibody. (b) HeLa-FcγRII cells
583 transiently expressing RFP-Rab10QL were infected with the indicated *L. pneumophila*
584 strains at an MOI of 10 for 1 h (see Figure 4-figure supplement 2). Rab10-positive LCVs
585 (%) were quantified. Infections were performed in triplicate and each value represents
586 scoring from 50 LCVs. Significance was determined using Student's t-test. (c) HEK293T-
587 FcγRII cells transiently expressing 3xFLAG-Rab10QL and HA-Ub were infected with
588 the *L. pneumophila* strains expressing Myc-tagged SdcB or its catalytic mutant for 7 h at
589 an MOI of 20. Rab10 was isolated from cell lysate by immunoprecipitation using anti-
590 FLAG magnetic beads and was probed with anti-FLAG and with anti-HA antibodies. For
591 detection of translocated SdcB, it was isolated from cell lysate by immunoprecipitation
592 using anti-Myc magnetic beads and was probed with anti-Myc antibody. Note that
593 apparent reduction of the wild-type SdcB was caused by its auto-ubiquitination leading
594 to the molecular weight shift (see text). (d, e) HeLa-FcγRII cells transiently expressing
595 RFP-Rab10 were infected with the indicated *L. pneumophila* strains at an MOI of 2 for
596 7h. (d) Representative images of infected cells. Fixed cells were stained for FLAG-SdcB
597 (green) and *L. pneumophila* (blue) and visualized with RFP-Rab10 (red). Magnified
598 images in the white squares are shown in each channel. White arrows indicate the position
599 of a bacterium. The red arrow indicates a Rab10 signal surrounding an LCV. Scale bars,
600 10 μm. (e) Quantitation of Rab10-positive LCVs (%) out of SdcB-positive ones.
601 Infections were performed in triplicate and each value represents scoring from 200 SdcB-
602 positive LCVs. Significance was determined using Student's t-test.
603 **Figure 5. The transglutaminase activity of MavC can mediate a unique Ub**

604 **conjugation to SdcB.**
605 (a) 3xFLAG-SdcB, HA-Ub and GFP-MavC were coexpressed in HEK293T-FcγRII cells.
606 SdcB was isolated from cell lysates by immunoprecipitation using anti-FLAG magnetic
607 beads and was probed with the indicated antibodies. The asterisks indicate the Ub-
608 conjugated form of SdcB. (b) 3xFLAG-SdcB and GFP-MavC were coexpressed in
609 HEK293T-FcγRII cells. SdcB was isolated from cell lysates by immunoprecipitation
610 using anti-FLAG magnetic beads and was probed with the indicated antibodies. The
611 asterisks indicate the Ub-conjugated form of SdcB. (c) *In vitro* transglutaminase assay
612 was performed using purified proteins. The samples were analyzed by SDS-PAGE
613 followed by silver staining (top) or by immunoblotting using the indicated antibodies
614 (middle and bottom). The asterisks indicate the Ub-conjugated form of SdcB. (d)
615 3xFLAG-SdcA or SidC, GFP-MavC and HA-Ub were coexpressed in HEK293T-FcγRII
616 cells. SdcA or SidC was isolated from cell lysates by immunoprecipitation using anti-
617 FLAG magnetic beads and was probed with the indicated antibodies. The asterisks
618 indicate the Ub-conjugated form of SdcA. (e) 3xFLAG-SdcB, GFP-MavC and HA-Ub or
619 Ub without any Lys residues ($Ub_{No\ K}$) were coexpressed in HEK293T-FcγRII cells. SdcB
620 was isolated from cell lysates by immunoprecipitation using anti-FLAG magnetic beads
621 and was probed with the indicated antibodies. The asterisks indicate the Ub-conjugated
622 form of SdcB. (f) 3xFLAG-SdcB, GFP-MavC and HA-Ub or Ub in which the C-terminal
623 GG were replaced with AA (Ub_{AA}) were coexpressed in HEK293T-FcγRII cells. SdcB
624 was isolated from cell lysates by immunoprecipitation using anti-FLAG magnetic beads
625 and was probed with the indicated antibodies. The asterisks indicate the Ub-conjugated
626 form of SdcB.
627
628 **Figure 6. Identification of residues on Ub and SdcB between which MavC can**
629 **crosslink.**
630 (a) MavC catalyzes the formation of an isopeptide bond between the Gln41 of Ub and the
631 Lys518 of SdcB. The indicated proteins were expressed in HEK293T-FcγRII cells and
632 SdcB was isolated from cell lysates by immunoprecipitation using anti-FLAG magnetic
633 beads. The samples were resolved by SDS-PAGE. The Ub-conjugated SdcB was detected
634 by immunoblotting and by CBB staining. The gel slices of areas of the bands shown with
635 the red squares were subjected to mass spectrometric analysis. Product ion spectrum was
636 shown for Ub peptide –AKIQDKEGIPPDQQR- crosslinked with SdcB peptide –
637 VLLDKEVNDEGIAEAVASK-. (b, c) The indicated proteins were coexpressed in
638 HEK293T-FcγRII cells. SdcB was isolated from cell lysates by immunoprecipitation
639 using anti-FLAG magnetic beads and was probed with the indicated antibodies. The

640 asterisks indicate the Ub-conjugated form of SdcB.
641
642 **Figure 7. Catalytic activity of MavC negatively regulates the Rab10 localization to**
643 **the LCV.**
644 (a, b) HeLa-FcγRII cells transiently expressing RFP-Rab10 and HA-MavC or its catalytic
645 mutant were infected with the Lp01 Δ*sidC*Δ*sdcA*Δ*sdcB* strain complemented with the
646 plasmid expressing 3xFLAG-SdcB or its catalytic mutant at an MOI of 2 for 4 h. (a)
647 Representative images of cells infected with the Lp01 Δ*sidC*Δ*sdcA*Δ*sdcB* strain
648 complemented with the plasmid expressing 3xFLAG-SdcB. Fixed cells were stained for
649 FLAG-SdcB (green) and DNA (blue), and visualized with RFP-Rab10 (red). Magnified
650 images in the white squares are shown in each channel. White arrows indicate the position
651 of a bacterium. The red arrow indicates a Rab10 signal surrounding an LCV. Scale bars,
652 10 μm. (b) Quantitation of Rab10-positive LCVs (%) out of SdcB-positive ones.
653 Infections were performed in triplicate and each value represents scoring from 200 SdcB-
654 positive LCVs. Significance was determined using Student's t-test. (c) HeLa-FcγRII cells
655 transiently expressing RFP-Rab10 were infected with the indicated Lp01 strains at an
656 MOI of 2 for 9 h, and Rab10-positive LCVs (%) were quantified. Infections were
657 performed in triplicate and each value represents scoring from 200 LCVs. Significance
658 was determined using Student's t-test. (d) The schematic of roles of SidE and SidC family
659 ligases in Rab10 localization to the LCV and of negative regulation of SdcB-dependent
660 Rab10 retention by the transglutaminase activity of MavC. Red arrows indicate canonical
661 Ub conjugation by SidC, SdcA and SdcB. Purple arrows indicate the noncanonical Ub
662 conjugation. In the early stage of infection, Rab10 is recruited and retained to the LCV.
663 This event is linked to its PR-ubiquitination catalyzed by the SidE effectors. The PR-
664 ubiquitination of Rab10 provides a platform of its polyubiquitination in a manner
665 depending on SidC and SdcA. In later stages, SdcB contributes towards sustained Ub
666 accumulation on the LCV, enabling the LCV to maintain Rab10 on the vacuole. MavC-
667 mediated crosslinking between Ub and SdcB disrupts the catalytic activity of SdcB,
668 eventually releasing Rab10 from the LCV.
669
670 **Figure 1-figure supplement 1. Mutation of Lys102, Lys136, and Lys154 on Rab10**
671 **did not eliminate ubiquitination of Rab10 upon infection.**
672 HEK293T-FcγRII cells transiently expressing 3xFLAG-Rab10 or 3xFLAG-Rab10 $_{K102A}$
673 $_{K136A\,L154A}$ (KKK) (a) with HA-Ub were infected with the indicated *L. pneumophila* strains
674 for 1 h (a) or 7 h (b) at an MOI of 20. Rab10 was isolated from cell lysate by
675 immunoprecipitation using anti-FLAG magnetic beads and was probed with anti-FLAG

676 and with anti-HA antibodies.
677
678 **Figure 4-figure supplement 1. Active Rab10 is preferentially targeted for infection-**
679 **induced ubiquitination.**
680 HEK293T-FcγRII cells transiently expressing 3xFLAG-Rab10 $_{Q68L}$ (QL) or Rab10 $_{T23N}$
681 (TN) with HA-Ub were infected with the wild-type *L. pneumophila* strain or treated with
682 media containing anti-*Legionella* antiserum (mock infection) for 1 h at an MOI of 20.
683 Rab10 was isolated from cell lysate by immunoprecipitation using anti-FLAG magnetic
684 beads and was probed with anti-FLAG and with anti-HA antibodies.
685
686 **Figure 4-figure supplement 2. The SidE- and SidC-family proteins contribute**
687 **towards retaining active Rab10 to the LCV.**
688 HeLa-FcγRII cells transiently expressing RFP-Rab10QL were infected with the indicated
689 *L. pneumophila* strains at an MOI of 10 for 1 h. Cells were fixed and stained with anti-
690 *Legionella* antiserum (green) before permeabilization of cells for detection of
691 extracellular bacteria. Permeabilized cells were stained with DAPI (blue) for detection of
692 intracellular bacteria (and nuclei) and with RFP-Rab10 (red). Representative images of
693 infected cells were shown. Magnified merged images in the white squares are shown as
694 enlarged images. Scale bars, 5 μm.
695
696 **Figure 5-figure supplement 1. SdcB has a catalytic activity of self-ubiquitination**
697 **with preference of various E2 enzymes.**
698 Ub, E1 enzyme, indicated E2 enzymes and purified His-SdcB or His-SidC were mixed in
699 the reaction buffer in the presence of ATP and incubated at 30°C for 120 min. The samples
700 were analyzed by SDS-PAGE followed by silver staining (top) or by immunoblotting
701 using the anti-Ub antibody (bottom).
702
703 **Figure 5-figure supplement 2. The catalytic activity of MavC negatively impacts on**
704 **auto-ubiquitination of SdcB.**
705 (a) 3xFLAG-SdcB, HA-Ub and GFP-MavC were coexpressed in HEK293T-FcγRII cells.
706 After 24 h transfection, cell media was replaced with media containing 10 μM of MG132
707 or equivalent amount of DMSO, and incubation of cells was resumed for additional 6 h.
708 The cell lysates were probed with the indicated antibodies. (b) The *in vitro* reaction was
709 performed with recombinant Ub, E1 enzyme, His-UbcH6, purified His-SdcB and His-
710 MavC in the reaction buffer in the presence of ATP by incubation at 30°C for 120 min.
711 The samples were analyzed by SDS-PAGE followed by immunoblotting using the anti-

712 Ub antibody.
713
714 **Figure 6-figure supplement 1. Mass spectrometry analysis identified additional**
715 **residues forming a covalent linkage between Ub and SdcB.**
716 Product ion spectrum was shown for Ub peptide –IQDKEGIPPDQQR- crosslinked with
717 SdcB peptide –GYVGVFFSGKENIK-.
718
719 **Figure 6-figure supplement 2. Mutations on Lys518 and Lys891 of SdcB did not**
720 **affect ubiquitination of Rab10.**
721 HEK293T-FcγRII cells transiently expressing 3xFLAG-Rab10QL and HA-Ub were
722 infected with the *L. pneumophila* Δ*sidC*Δ*sdcA*Δ*sdcB* strain expressing Myc-tagged SdcB,
723 its catalytic mutant (SdcB $_{C57A}$) or SdcB $_{K518R\ K891R}$ for 7 h at an MOI of 20. Rab10 was
724 isolated from cell lysate by immunoprecipitation using anti-FLAG magnetic beads and
725 was probed with anti-FLAG and with anti-HA antibodies. For detection of translocated
726 SdcB, it was isolated from cell lysate by immunoprecipitation using anti-Myc magnetic
727 beads and was probed with anti-Myc antibody. Note that apparent loss of SdcB was
728 caused by its auto-ubiquitination leading to the molecular weight shift.
729
730 **Figure 7-figure supplement 1. Bacterially delivered MavC mediates elimination of**
731 **Rab10 from the LCV.**
732 Representative images of cells infected with the indicated Lp01 strains at an MOI of 2 for
733 9 h (Rab10-positive LCVs (%) were quantified in Figure 7c). Fixed cells were stained for
734 *L. pneumophila* (green) and DNA (blue), and visualized with RFP-Rab10 (red).
735 Magnified images in the white squares are shown in each channel. Red arrows indicate
736 the Rab10 signal surrounding an LCV. Scale bars, 10 μm.
737
738 **Figure 7-figure supplement 2. Ectopic expression of SdcB does not proceed Rab10**
739 **polyubiquitination even in the presence of SdeA.**
740 Indicated proteins were coexpressed in HEK293T-FcγRII cells. Rab10 was isolated from
741 cell lysates by immunoprecipitation using anti-RFP magnetic beads and was probed with
742 the indicated antibodies. The asterisks indicate the Ub-conjugated form of Rab10.
743
744
745 **Ethics statement**
746 Not applicable.
747

QUANTIFICATION AND STATISTICAL ANALYSIS

In the immunofluorescence experiments, at least 50 bacterial vacuoles were counted per experiment. Student's t tests were carried out with data from three independent experiments.

References

Arasaki K, Mikami Y, Shames SR, Inoue H, Wakana Y, Tagaya M. 2017. Legionella effector Lpg1137 shuts down ER-mitochondria communication through cleavage of syntaxin 17. *Nat Commun* **8**. doi:10.1038/ncomms15406

Arasaki K, Roy CR. 2010. Legionella pneumophila promotes functional interactions between plasma membrane syntaxins and Sec22b. *Traffic* **11**:587–600. doi:10.1111/j.1600-0854.2010.01050.x

Arasaki K, Toomre DK, Roy CR. 2012. The legionella pneumophila effector DrrA is sufficient to stimulate SNARE-dependent membrane fusion. *Cell Host Microbe* **11**:46–57. doi:10.1016/j.chom.2011.11.009

Ashida H, Sasakawa C. 2017. Bacterial E3 ligase effectors exploit host ubiquitin systems. *Curr Opin Microbiol*. doi:10.1016/j.mib.2016.11.001

Berger KH, Merriam JJ, Isberg RR. 1994. Altered intracellular targeting properties associated with mutations in the Legionella pneumophila dotA gene. *Mol Microbiol* **14**:809–822. doi:10.1111/j.1365-2958.1994.tb01317.x

Bhogaraju S, Kalayil S, Liu Y, Bonn F, Colby T, Matic I, Dikic I. 2016. Phosphoribosylation of Ubiquitin Promotes Serine Ubiquitination and Impairs Conventional Ubiquitination. *Cell* **167**:1636-1649.e13. doi:10.1016/j.cell.2016.11.019

Black MH, Osinski A, Gradowski M, Servage KA, Pawłowski K, Tomchick DR, Tagliabracci VS. 2019. Bacterial pseudokinase catalyzes protein polyglutamylation to inhibit the SidE-family ubiquitin ligases. *Science* **364**:787–792. doi:10.1126/science.aaw7446

Feeley JC, Gibson RJ, Gorman GW, Langford NC, Rasheed JK, Mackel DC, Baine WB. 1979. Charcoal-yeast extract agar: primary isolation medium for Legionella pneumophila. *J Clin Microbiol* **10**:437–441. doi:10.1128/jcm.10.4.437-441.1979

Gan N, Guan H, Huang Y, Yu T, Fu J, Nakayasu ES, Puvar K, Das C, Wang D, Ouyang S, Luo Z. 2020. Legionella pneumophila regulates the activity of UBE 2N by deamidase-mediated deubiquitination. *EMBO J* **39**. doi:10.15252/embj.2019102806

Gan N, Nakayasu ES, Hollenbeck PJ, Luo ZQ. 2019a. Legionella pneumophila inhibits immune signalling via MavC-mediated transglutaminase-induced ubiquitination of

UBE2N. *Nat Microbiol* **4**:134–143. doi:10.1038/s41564-018-0282-8

Gan N, Zhen X, Liu Yao, Xu X, He C, Qiu J, Liu Yancheng, Fujimoto GM, Nakayasu ES, Zhou B, Zhao L, Puvar K, Das C, Ouyang S, Luo ZQ. 2019b. Regulation of phosphoribosyl ubiquitination by a calmodulin-dependent glutamylase. *Nature* **572**:387–391. doi:10.1038/s41586-019-1439-1

Guan H, Fu J, Yu T, Wang ZX, Gan N, Huang Y, Perčulija V, Li Y, Luo ZQ, Ouyang S. 2020. Molecular Basis of Ubiquitination Catalyzed by the Bacterial Transglutaminase MavC. *Advanced Science* **7**. doi:10.1002/advs.202000871

Horenkamp FA, Mukherjee S, Alix E, Schauder CM, Hubber AM, Roy CR, Reinisch KM. 2014. Legionella pneumophila subversion of host vesicular transport by SidC effector proteins. *Traffic* **15**:488–499. doi:10.1111/tra.12158

Hsu FS, Luo X, Qiu J, Teng Y Bin, Jin J, Smolka MB, Luo ZQ, Mao Y. 2014. The Legionella effector SidC defines a unique family of ubiquitin ligases important for bacterial phagosomal remodeling. *Proc Natl Acad Sci U S A* **111**:10538–10543. doi:10.1073/pnas.1402605111

Hubber A, Roy CR. 2010. Modulation of host cell function by legionella pneumophila type IV effectors. *Annu Rev Cell Dev Biol*. doi:10.1146/annurev-cellbio-100109-104034

Ingmundson A, Delprato A, Lambright DG, Roy CR. 2007. Legionella pneumophila proteins that regulate Rab1 membrane cycling. *Nature* **450**:365–369. doi:10.1038/nature06336

Isberg RR, O'Connor TJ, Heidtman M. 2009. The Legionella pneumophila replication vacuole: Making a cosy niche inside host cells. *Nat Rev Microbiol*. doi:10.1038/nrmicro1967

Jeng EE, Bhadkamkar V, Ibe NU, Gause H, Jiang L, Chan J, Jian R, Jimenez-Morales D, Stevenson E, Krogan NJ, Swaney DL, Snyder MP, Mukherjee S, Bassik MC. 2019. Systematic Identification of Host Cell Regulators of Legionella pneumophila Pathogenesis Using a Genome-wide CRISPR Screen. *Cell Host Microbe* **26**:551-563.e6. doi:10.1016/j.chom.2019.08.017

Kagan JC, Stein MP, Pypaert M, Roy CR. 2004. Legionella Subvert the Functions of Rab1 and Sec22b to Create a Replicative Organelle. *Journal of Experimental Medicine* **199**:1201–1211. doi:10.1084/jem.20031706

Kalayil S, Bhogaraju S, Bonn F, Shin D, Liu Y, Gan N, Basquin J, Grumati P, Luo ZQ, Dikic I. 2018. Insights into catalysis and function of phosphoribosyl-linked serine ubiquitination. *Nature* **557**:734–738. doi:10.1038/s41586-018-0145-8

Kawabata M, Matsuo H, Koito T, Murata M, Kubori T, Nagai H, Tagaya M, Arasaki K.

2021. Legionella hijacks the host Golgi-to-ER retrograde pathway for the association of Legionella-containing vacuole with the ER. *PLoS Pathog* **17**. doi:10.1371/JOURNAL.PPAT.1009437

Kitao T, Nagai H, Kubori T. 2020. Divergence of Legionella Effectors Reversing Conventional and Unconventional Ubiquitination. *Front Cell Infect Microbiol*. doi:10.3389/fcimb.2020.00448

Kotewicz KM, Ramabhadran V, Sjoblom N, Vogel JP, Haenssler E, Zhang M, Behringer J, Scheck RA, Isberg RR. 2017. A Single Legionella Effector Catalyzes a Multistep Ubiquitination Pathway to Rearrange Tubular Endoplasmic Reticulum for Replication. *Cell Host Microbe* **21**:169–181. doi:10.1016/j.chom.2016.12.007

Kubori T, Kitao T, Ando H, Nagai H. 2018. LotA, a Legionella deubiquitinase, has dual catalytic activity and contributes to intracellular growth. *Cell Microbiol* **20**. doi:10.1111/cmi.12840

Kubori T, Kitao T, Nagai H. 2019. Emerging insights into bacterial deubiquitinases. *Curr Opin Microbiol*. doi:10.1016/j.mib.2018.10.001

Kubori T, Nagai H. 2016. The Type IVB secretion system: An enigmatic chimera. *Curr Opin Microbiol*. doi:10.1016/j.mib.2015.10.001

Lin YH, Lucas M, Evans TR, Abascal-Palacios G, Doms AG, Beauchene NA, Rojas AL, Hierro A, Machner MP. 2018. RavN is a member of a previously unrecognized group of Legionella pneumophila E3 ubiquitin ligases. *PLoS Pathog* **14**. doi:10.1371/journal.ppat.1006897

Lin YH, Machner MP. 2017. Exploitation of the host cell ubiquitin machinery by microbial effector proteins. *J Cell Sci*. doi:10.1242/jcs.188482

Liu S, Luo J, Zhen X, Qiu J, Ouyang S, Luo ZQ. 2020. Interplay between bacterial deubiquitinase and ubiquitin e3 ligase regulates ubiquitin dynamics on legionella phagosomes. *Elife* **9**:1–23. doi:10.7554/eLife.58114

Luo J, Wang L, Song L, Luo ZQ. 2021. Exploitation of the Host Ubiquitin System: Means by Legionella pneumophila. *Front Microbiol*. doi:10.3389/fmicb.2021.790442

Luo X, Wasilko DJ, Liu Y, Sun J, Wu X, Luo ZQ, Mao Y. 2015. Structure of the Legionella Virulence Factor, SidC Reveals a Unique PI(4)P-Specific Binding Domain Essential for Its Targeting to the Bacterial Phagosome. *PLoS Pathog* **11**. doi:10.1371/journal.ppat.1004965

Machner MP, Isberg RR. 2006. Targeting of Host Rab GTPase Function by the Intravacuolar Pathogen Legionella pneumophila. *Dev Cell* **11**:47–56. doi:10.1016/j.devcel.2006.05.013

Meier F, Beck S, Grassl N, Lubeck M, Park MA, Raether O, Mann M. 2015. Parallel

accumulation-serial fragmentation (PASEF): Multiplying sequencing speed and sensitivity by synchronized scans in a trapped ion mobility device. *J Proteome Res* **14**:5378–5387. doi:10.1021/acs.jproteome.5b00932

Meier F, Brunner AD, Koch S, Koch H, Lubeck M, Krause M, Goedecke N, Decker J, Kosinski T, Park MA, Bache N, Hoerning O, Cox J, Räther O, Mann M. 2018. Online parallel accumulation–serial fragmentation (PASEF) with a novel trapped ion mobility mass spectrometer. *Molecular and Cellular Proteomics* **17**:2534–2545. doi:10.1074/mcp.TIR118.000900

Mukherjee S, Liu X, Arasaki K, McDonough J, Galán JE, Roy CR. 2011. Modulation of Rab GTPase function by a protein phosphocholine transferase. *Nature* **477**:103–108. doi:10.1038/nature10335

Müller MP, Peters H, Blümer J, Blankenfeldt W, Goody RS, Itzen A. 2010. The Legionella Effector Protein DrrA AMPylates the Membrane Traffic Regulator Rab1b. *Science (1979)* **329**:946–949. doi:10.1126/science.1192276

Murata T, Delprato A, Ingmundson A, Toomre DK, Lambright DG, Roy CR. 2006. The Legionella pneumophila effector protein DrrA is a Rab1 guanine nucleotide-exchange factor. *Nat Cell Biol* **8**:971–977. doi:10.1038/ncb1463

Neunuebel MR, Chen Y, Gaspar AH, Backlund PS, Yergey A, Machner MP. 2011. De-AMPylation of the Small GTPase Rab1 by the Pathogen Legionella pneumophila. *Science (1979)* **333**:453–456. doi:10.1126/science.1207193

Neunuebel MR, Machner MP. 2012. The taming of a Rab GTPase by Legionella pneumophila. *Small GTPases* **3**:28–33. doi:10.4161/sgtp.18704

Puvar K, Iyer S, Fu J, Kenny S, Negrón Terón KI, Luo ZQ, Brzovic PS, Klevit RE, Das C. 2020. Legionella effector MavC targets the Ube2N~Ub conjugate for noncanonical ubiquitination. *Nat Commun* **11**. doi:10.1038/s41467-020-16211-x

Qiu J, Luo ZQ. 2017. Legionella and Coxiella effectors: Strength in diversity and activity. *Nat Rev Microbiol*. doi:10.1038/nrmicro.2017.67

Qiu J, Sheedlo MJ, Yu K, Tan Y, Nakayasu ES, Das C, Liu X, Luo ZQ. 2016. Ubiquitination independent of E1 and E2 enzymes by bacterial effectors. *Nature* **533**:120–124. doi:10.1038/nature17657

Qiu J, Yu K, Fei X, Liu Y, Nakayasu ES, Piehowski PD, Shaw JB, Puvar K, Das C, Liu X, Luo ZQ. 2017. A unique deubiquitinase that deconjugates phosphoribosyl-linked protein ubiquitination. *Cell Res* **27**:865–881. doi:10.1038/cr.2017.66

Ragaz C, Pietsch H, Urwyler S, Tiaden A, Weber SS, Hilbi H. 2008. The Legionella pneumophila phosphatidylinositol-4 phosphate-binding type IV substrate SidC recruits endoplasmic reticulum vesicles to a replication-permissive vacuole. *Cell*

892 *Microbiol* **10**:2416–2433. doi:10.1111/j.1462-5822.2008.01219.x
893 Sherwood RK, Roy CR. 2013. A rab-centric perspective of bacterial pathogen-occupied
894 vacuoles. *Cell Host Microbe*. doi:10.1016/j.chom.2013.08.010
895 Shin D, Mukherjee R, Liu Yaobin, Gonzalez A, Bonn F, Liu Yan, Rogov V V., Heinz M,
896 Stolz A, Hummer G, Dötsch V, Luo ZQ, Bhogaraju S, Dikic I. 2020. Regulation of
897 Phosphoribosyl-Linked Serine Ubiquitination by Deubiquitinases DupA and DupB.
898 *Mol Cell* **77**:164-179.e6. doi:10.1016/j.molcel.2019.10.019
899 Spanò S, Galán JE. 2018. Taking control: Hijacking of Rab GTPases by intracellular
900 bacterial pathogens. *Small GTPases*. doi:10.1080/21541248.2017.1336192
901 Sulpizio A, Minelli ME, Wan M, Burrowes PD, Wu X, Sanford EJ, Shin J-H, Williams
902 BC, Goldberg ML, Smolka MB, Mao Y. 2019. Protein polyglutamylation catalyzed
903 by the bacterial calmodulin-dependent pseudokinase SidJ. *Elife* **8**:e51162.
904 doi:10.7554/eLife.51162.001
905 Tan Y, Luo ZQ. 2011. Legionella pneumophila SidD is a deAMPylase that modifies Rab1.
906 *Nature* **475**:506–509. doi:10.1038/nature10307
907 Tomaskovic I, Gonzalez A, Dikic I. 2022. Ubiquitin and Legionella: From bench to
908 bedside. *Semin Cell Dev Biol*. doi:10.1016/j.semcdb.2022.02.008
909 Urbanus ML, Quaile AT, Stogios PJ, Morar M, Rao C, Di Leo R, Evdokimova E, Lam M,
910 Oatway C, Cuff ME, Osipiuk J, Michalska K, Nocek BP, Taipale M, Savchenko A,
911 Ensminger AW. 2016. Diverse mechanisms of metaeffector activity in an
912 intracellular bacterial pathogen, Legionella pneumophila. *Mol Syst Biol* **12**:893.
913 doi:10.15252/msb.20167381
914 Valleau D, Quaile AT, Cui H, Xu X, Evdokimova E, Chang C, Cuff ME, Urbanus ML,
915 Houliston S, Arrowsmith CH, Ensminger AW, Savchenko A. 2018. Discovery of
916 Ubiquitin Deamidases in the Pathogenic Arsenal of Legionella pneumophila. *Cell*
917 *Rep* **23**:568–583. doi:10.1016/j.celrep.2018.03.060
918 Vormittag S, Hüsler D, Haneburger I, Kroniger T, Anand A, Prantl M, Barisch C, Maaß
919 S, Becher D, Letourneur F, Hilbi H. 2023. Legionella - and host-driven lipid flux at
920 LCV-ER membrane contact sites promotes vacuole remodeling. *EMBO Rep* **24**.
921 doi:10.15252/embr.202256007
922 Zuckman DM, Hung JB, Roy CR. 1999. Pore-forming activity is not sufficient for
923 Legionella pneumophila phagosome trafficking and intracellular growth. *Mol*
924 *Microbiol* **32**:990–1001. doi:10.1046/j.1365-2958.1999.01410.x
925

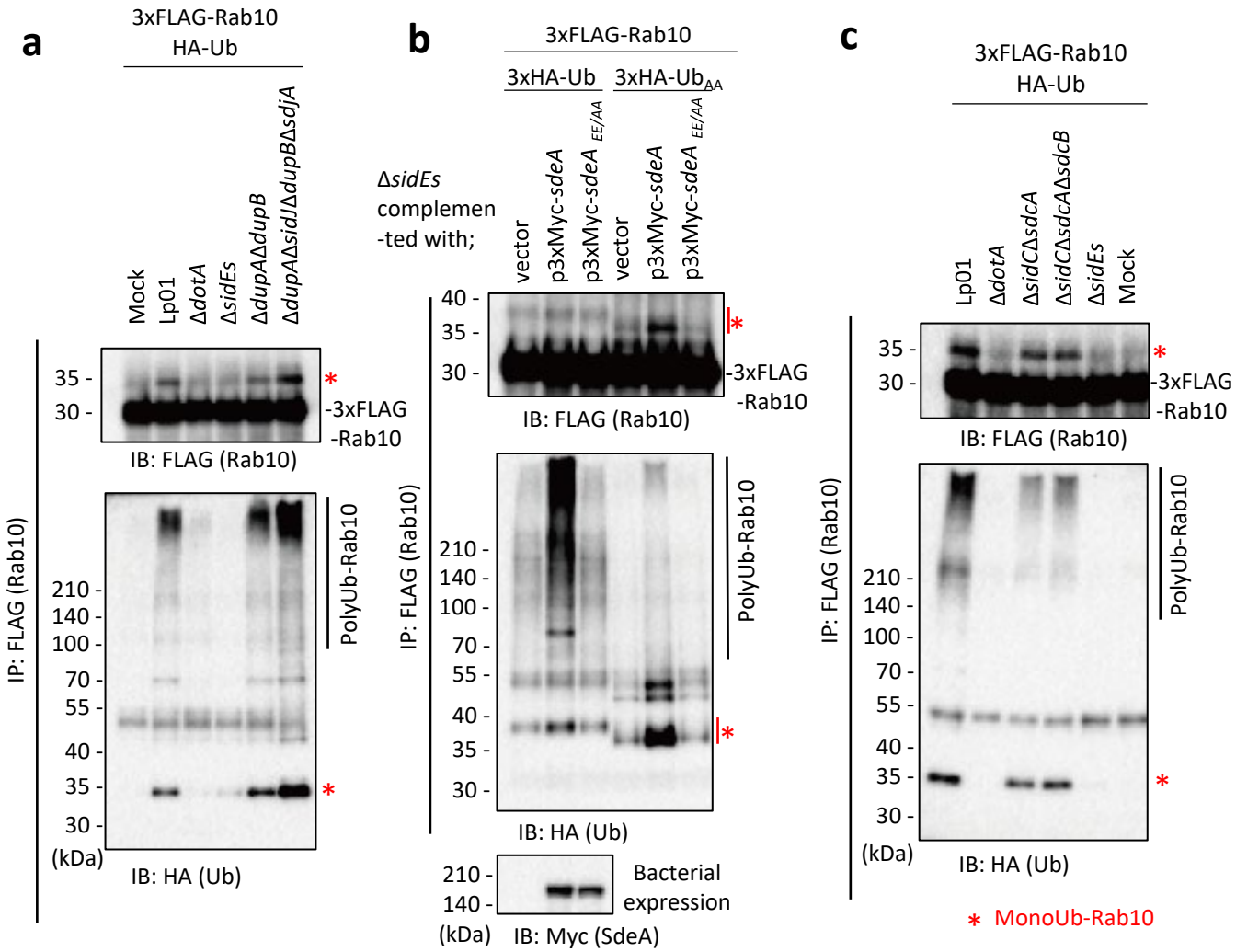
a
3xFLAG-Rab10
HA-Ub
Mock
Lp01
ΔdotA
ΔsidEs
ΔdupAΔdupB
ΔdupAΔsidJΔdupBΔsdjA
35 -
30 -
-3xFLAG
-Rab10
IB: FLAG (Rab10)
IP: FLAG (Rab10)
210 -
140 -
100 -
70 -
55 -
40 -
35 -
30 -
(kDa)
PolyUb-Rab10
IB: HA (Ub)
b
3xFLAG-Rab10
3xHA-Ub
3xHA-Ub$_{\Delta A}$
ΔsidEs
complemen
-ted with;
vector
p3xMyc-sdeA
p3xMyc-sdeA EE/AA
vector
p3xMyc-sdeA
p3xMyc-sdeA EE/AA
40 -
35 -
30 -
-3xFLAG
-Rab10
IB: FLAG (Rab10)
IP: FLAG (Rab10)
210 -
140 -
100 -
70 -
55 -
40 -
35 -
30 -
PolyUb-Rab10
IB: HA (Ub)
210 -
140 -
(kDa)
Bacterial
expression
IB: Myc (SdeA)
c
3xFLAG-Rab10
HA-Ub
Lp01
ΔdotA
ΔsidCΔsdcA
ΔsidCΔsdcAΔsdcB
ΔsidEs
Mock
35 -
30 -
-3xFLAG
-Rab10
IB: FLAG (Rab10)
IP: FLAG (Rab10)
210 -
140 -
100 -
70 -
55 -
40 -
35 -
30 -
(kDa)
PolyUb-Rab10
IB: HA (Ub)
* MonoUb-Rab10

Figure 1

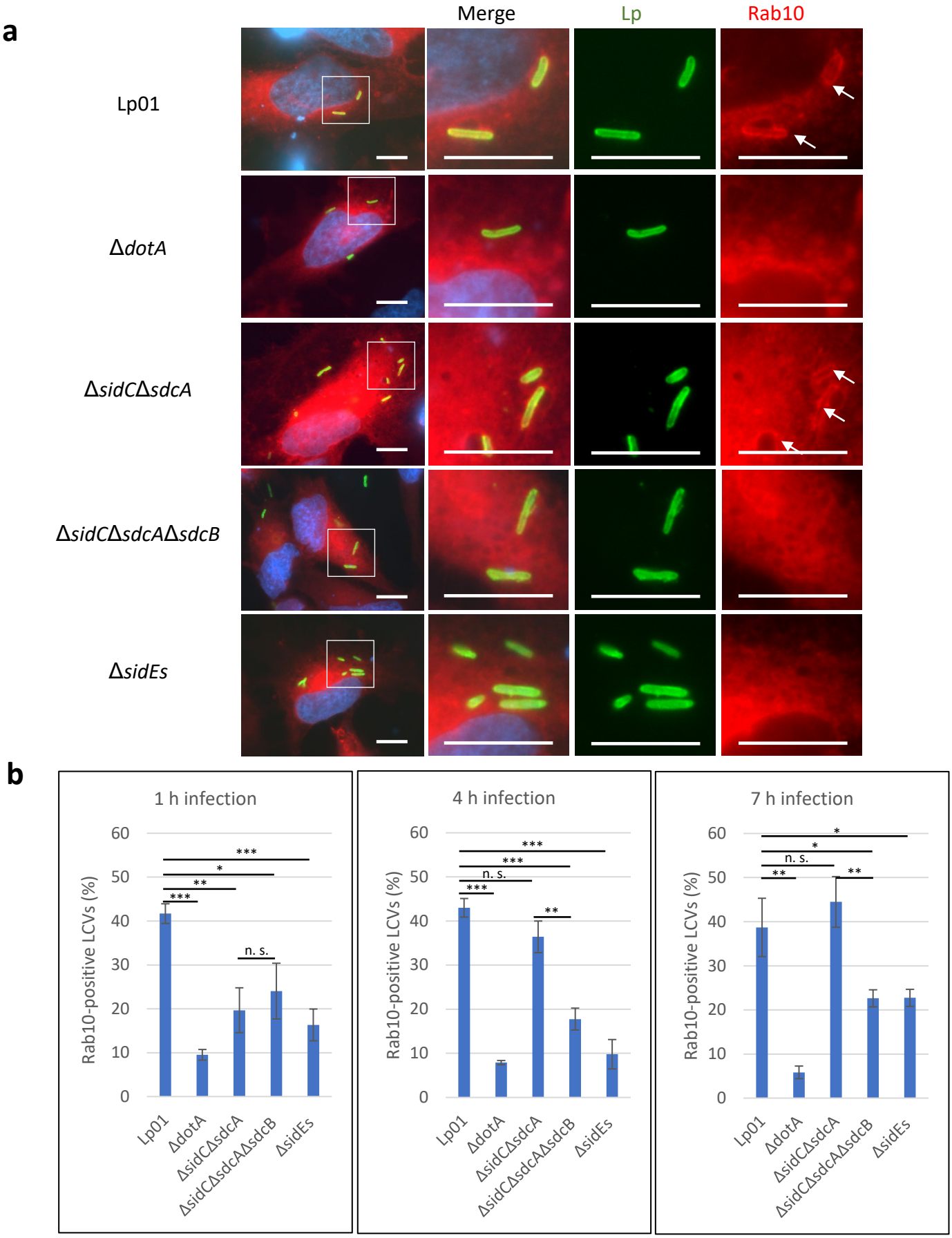
a
Merge
Lp
Rab10
Lp01
ΔdotA
ΔsidCΔsdcA
ΔsidCΔsdcAΔsdcB
ΔsidEs
b
1 h infection
4 h infection
7 h infection
Rab10-positive LCVs (%)
0
10
20
30
40
50
60
***
*
**
n. s.
Lp01
ΔdotA
ΔsidCΔsdcA
ΔsidCΔsdcAΔsdcB
ΔsidEs
* p < 0.02
** p < 0.005
*** p < 0.001

Figure 2

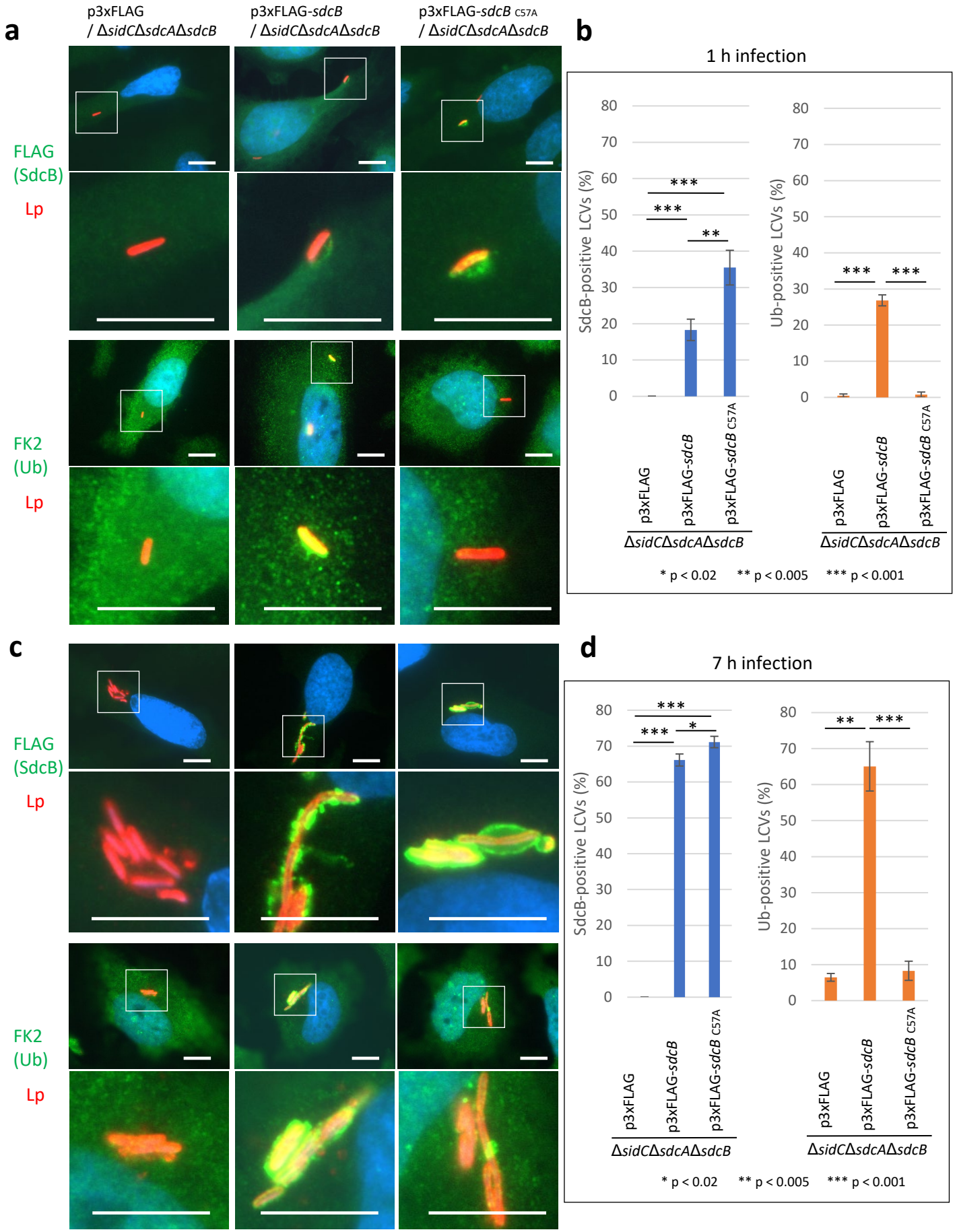
a
p3xFLAG / ΔsidCΔsdcAΔsdcB
p3xFLAG-sdcB / ΔsidCΔsdcAΔsdcB
p3xFLAG-sdcB C57A / ΔsidCΔsdcAΔsdcB
FLAG (SdcB)
Lp
FK2 (Ub)
Lp
b
1 h infection
SdcB-positive LCVs (%)
Ub-positive LCVs (%)
p3xFLAG
p3xFLAG-sdcB
p3xFLAG-sdcB C57A
ΔsidCΔsdcAΔsdcB
* p < 0.02 ** p < 0.005 *** p < 0.001
c
FLAG (SdcB)
Lp
FK2 (Ub)
Lp
d
7 h infection
SdcB-positive LCVs (%)
Ub-positive LCVs (%)
p3xFLAG
p3xFLAG-sdcB
p3xFLAG-sdcB C57A
ΔsidCΔsdcAΔsdcB
* p < 0.02 ** p < 0.005 *** p < 0.001

Figure 3

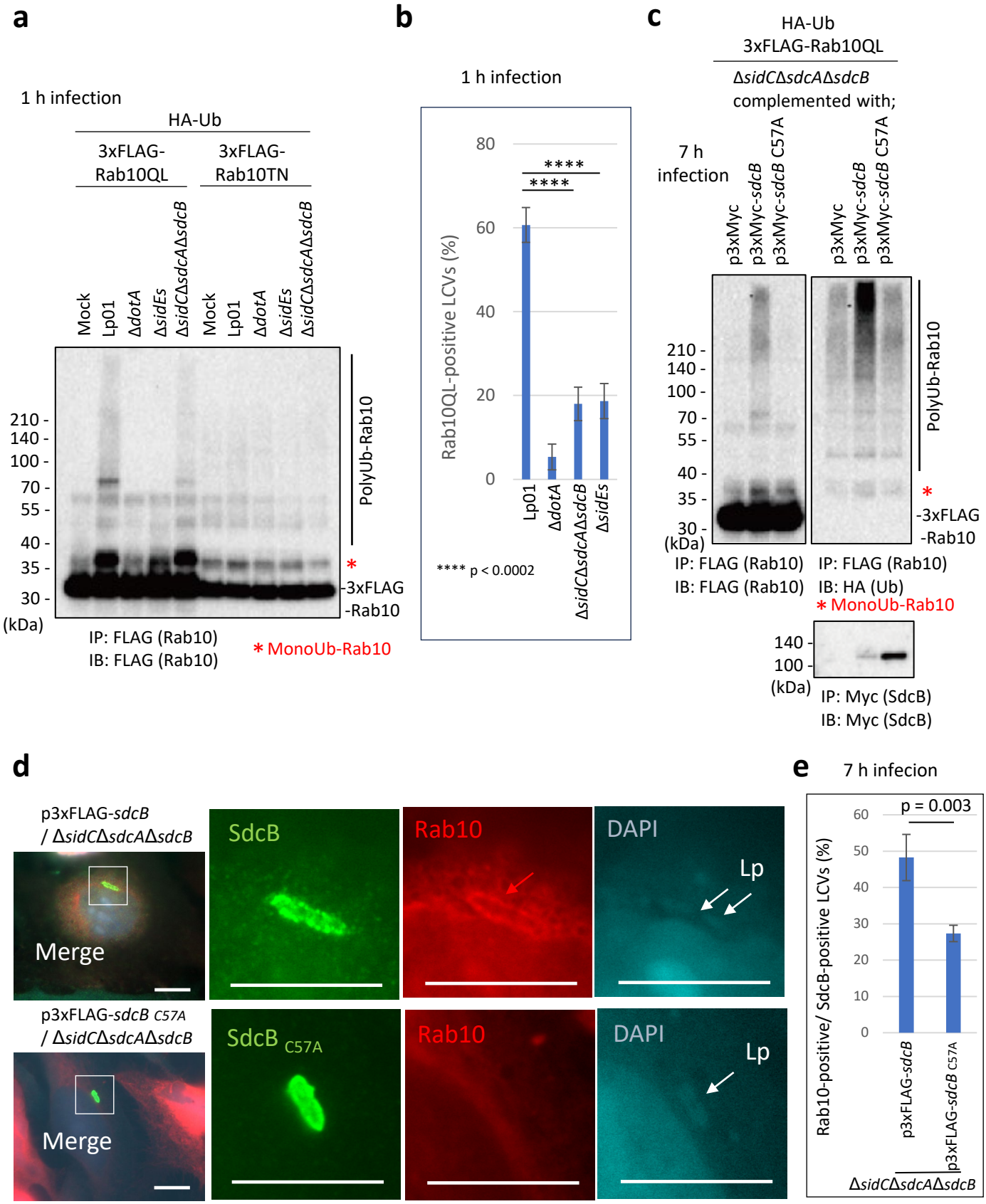
a
1 h infection
HA-Ub
3xFLAG-Rab10QL
3xFLAG-Rab10TN
Mock
Lp01
ΔdotA
ΔsidEs
ΔsidCΔsdcAΔsdcB
210 -
140 -
100 -
70 -
55 -
40 -
35 -
30 -
(kDa)
PolyUb-Rab10
*
-3xFLAG
-Rab10
IP: FLAG (Rab10)
IB: FLAG (Rab10)
* MonoUb-Rab10
b
1 h infection
Rab10QL-positive LCVs (%)
80
60
40
20
0
****
****
Lp01
ΔdotA
ΔsidCΔsdcAΔsdcB
ΔsidEs
**** p < 0.0002
c
HA-Ub
3xFLAG-Rab10QL
ΔsidCΔsdcAΔsdcB
complemented with;
7 h infection
p3xMyc
p3xMyc-sdcB
p3xMyc-sdcB C57A
210 -
140 -
100 -
70 -
55 -
40 -
35 -
30 -
(kDa)
PolyUb-Rab10
*
-3xFLAG
-Rab10
IP: FLAG (Rab10)
IB: FLAG (Rab10)
IP: FLAG (Rab10)
IB: HA (Ub)
* MonoUb-Rab10
140 -
100 -
(kDa)
IP: Myc (SdcB)
IB: Myc (SdcB)
d
p3xFLAG-sdcB
/ ΔsidCΔsdcAΔsdcB
Merge
SdcB
Rab10
DAPI
Lp
p3xFLAG-sdcB C57A
/ ΔsidCΔsdcAΔsdcB
Merge
SdcB C57A
Rab10
DAPI
Lp
e
7 h infecion
p = 0.003
Rab10-positive/ SdcB-positive LCVs (%)
60
50
40
30
20
10
0
p3xFLAG-sdcB
p3xFLAG-sdcB C57A
ΔsidCΔsdcAΔsdcB

Figure 4

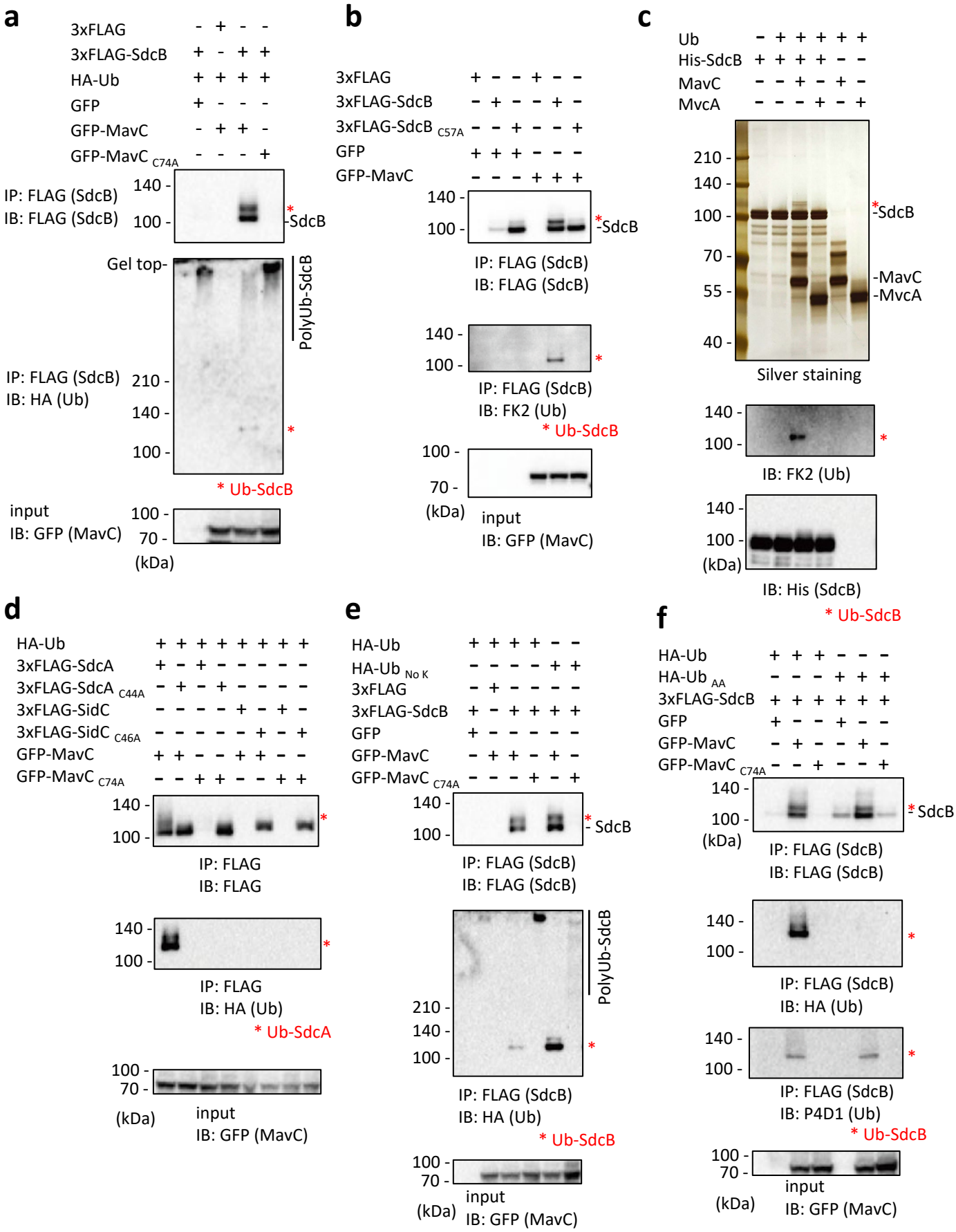
a
3xFLAG - + - -
3xFLAG-SdcB + - + +
HA-Ub + + + +
GFP + - - -
GFP-MavC - + + -
GFP-MavC C74A - - - +
IP: FLAG (SdcB)
IB: FLAG (SdcB)
140 -
100 -
* -SdcB
Gel top-
PolyUb-SdcB
IP: FLAG (SdcB)
IB: HA (Ub)
210 -
140 -
100 -
*
* Ub-SdcB
input
IB: GFP (MavC)
100 -
70 -
(kDa)
b
3xFLAG + - - + - -
3xFLAG-SdcB - + - - + -
3xFLAG-SdcB C57A - - + - - +
GFP + + + - - -
GFP-MavC - - - + + +
140 -
100 -
* -SdcB
IP: FLAG (SdcB)
IB: FLAG (SdcB)
140 -
100 -
*
IP: FLAG (SdcB)
IB: FK2 (Ub)
* Ub-SdcB
100 -
70 -
(kDa)
input
IB: GFP (MavC)
c
Ub - + + + + +
His-SdcB + + + + - -
MavC - - + - + -
MvcA - - - + - +
210 -
140 -
100 -
70 -
55 -
40 -
*SdcB
-MavC
-MvcA
Silver staining
140 -
100 -
*
IB: FK2 (Ub)
140 -
100 -
(kDa)
IB: His (SdcB)
* Ub-SdcB
d
HA-Ub + + + + + + + +
3xFLAG-SdcA + - + - - - - -
3xFLAG-SdcA C44A - + - + - - - -
3xFLAG-SidC - - - - + - + -
3xFLAG-SidC C46A - - - - - + - +
GFP-MavC + + - - + + - -
GFP-MavC C74A - - + + - - + +
140 -
100 -
*
IP: FLAG
IB: FLAG
140 -
100 -
*
IP: FLAG
IB: HA (Ub)
* Ub-SdcA
100 -
70 -
(kDa)
input
IB: GFP (MavC)
e
HA-Ub + + + + - -
HA-Ub No K - - - - + +
3xFLAG - + - - - -
3xFLAG-SdcB + - + + + +
GFP + - - - - -
GFP-MavC - + + - + -
GFP-MavC C74A - - - + - +
140 -
100 -
* SdcB
IP: FLAG (SdcB)
IB: FLAG (SdcB)
PolyUb-SdcB
210 -
140 -
100 -
*
IP: FLAG (SdcB)
IB: HA (Ub)
* Ub-SdcB
100 -
70 -
(kDa)
input
IB: GFP (MavC)
f
HA-Ub + + + - - -
HA-Ub AA - - - + + +
3xFLAG-SdcB + + + + + +
GFP + - - + - -
GFP-MavC - + - - + -
GFP-MavC C74A - - + - - +
140 -
100 -
(kDa)
* SdcB
IP: FLAG (SdcB)
IB: FLAG (SdcB)
140 -
100 -
*
IP: FLAG (SdcB)
IB: HA (Ub)
140 -
100 -
*
IP: FLAG (SdcB)
IB: P4D1 (Ub)
* Ub-SdcB
100 -
70 -
(kDa)
input
IB: GFP (MavC)

Figure 5

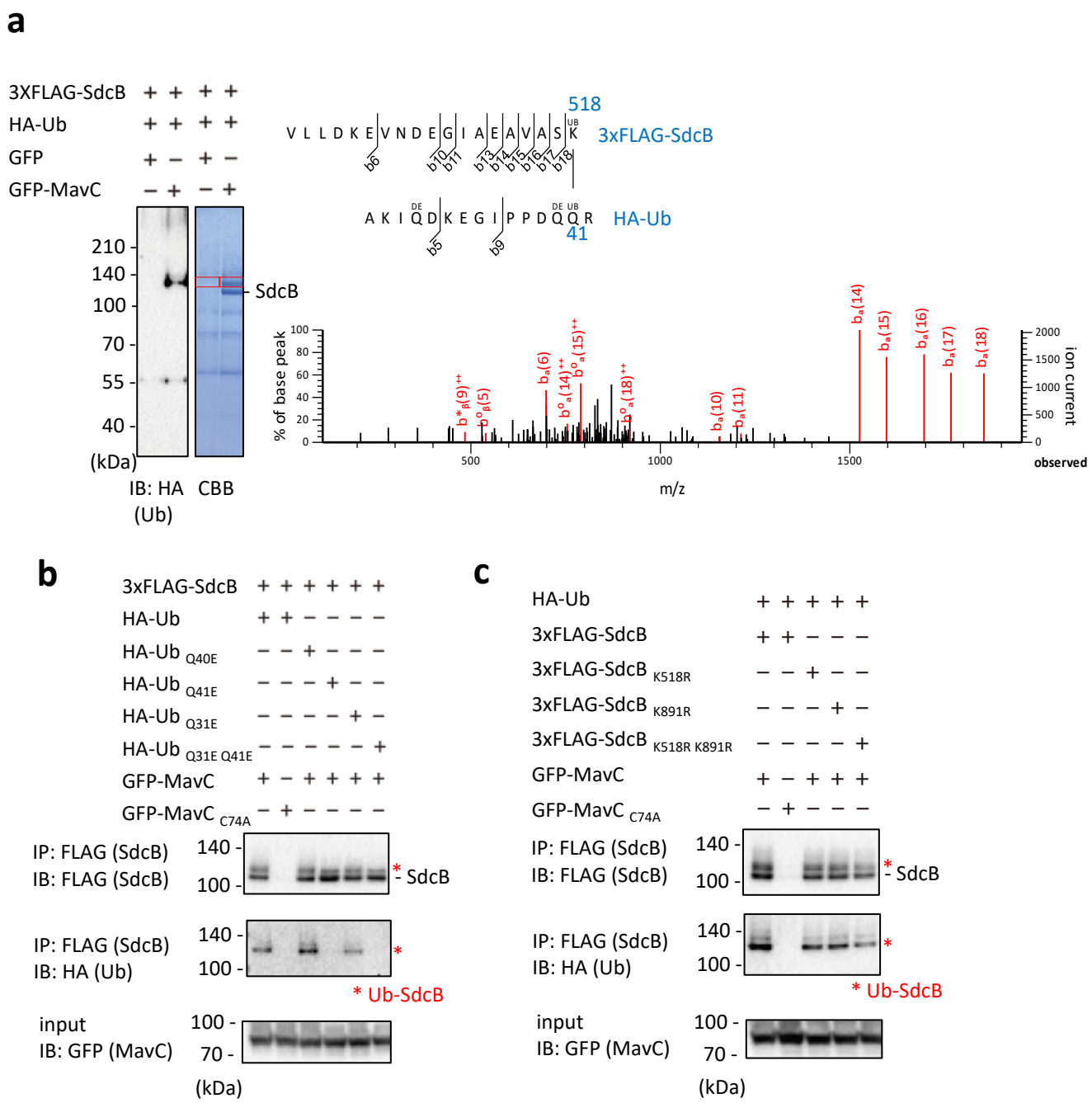
a
3XFLAG-SdcB + + + +
HA-Ub + + + +
GFP + − + −
GFP-MavC − + − +
210
140
100
70
55
40
(kDa)
SdcB
IB: HA (Ub)
CBB
518
V L L D K E V N D E G I A E A V A S K
3xFLAG-SdcB
A K I Q D K E G I P P D Q Q R
HA-Ub
41
% of base peak
m/z
ion current
observed
b
3xFLAG-SdcB + + + + + +
HA-Ub + + − − − −
HA-Ub Q40E − − + − − −
HA-Ub Q41E − − − + − −
HA-Ub Q31E − − − − + −
HA-Ub Q31E Q41E − − − − − +
GFP-MavC + − + + + +
GFP-MavC C74A − + − − − −
IP: FLAG (SdcB)
IB: FLAG (SdcB)
- SdcB
IP: FLAG (SdcB)
IB: HA (Ub)
* Ub-SdcB
input
IB: GFP (MavC)
(kDa)
c
HA-Ub + + + + +
3xFLAG-SdcB + + − − −
3xFLAG-SdcB K518R − − + − −
3xFLAG-SdcB K891R − − − + −
3xFLAG-SdcB K518R K891R − − − − +
GFP-MavC + − + + +
GFP-MavC C74A − + − − −
IP: FLAG (SdcB)
IB: FLAG (SdcB)
- SdcB
IP: FLAG (SdcB)
IB: HA (Ub)
* Ub-SdcB
input
IB: GFP (MavC)
(kDa)

Figure 6

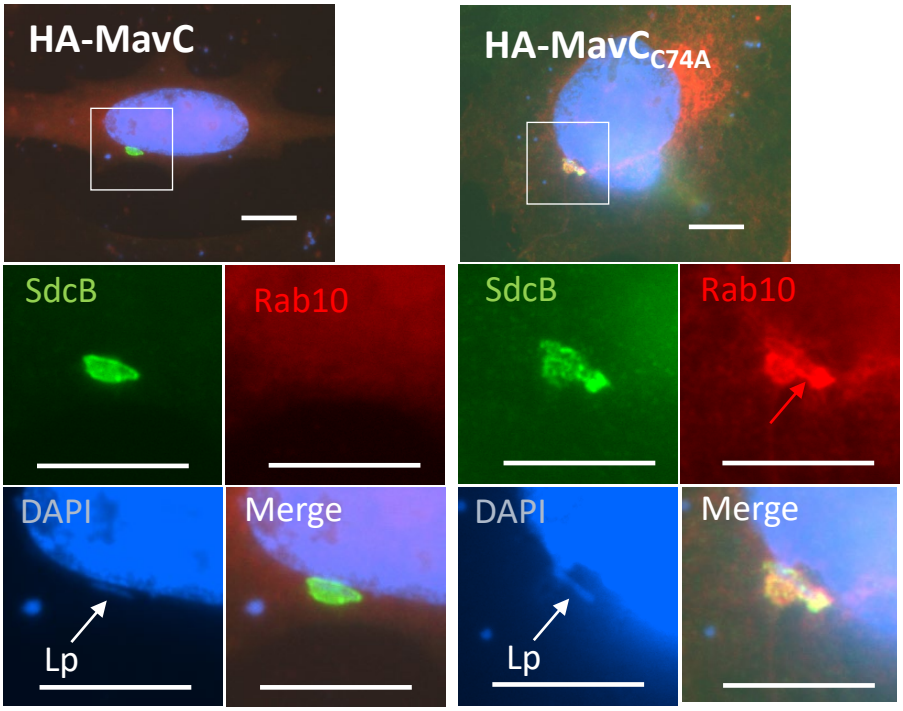
a
HA-MavC
HA-MavC C74A
SdcB
Rab10
SdcB
Rab10
DAPI
Merge
DAPI
Merge
Lp
Lp

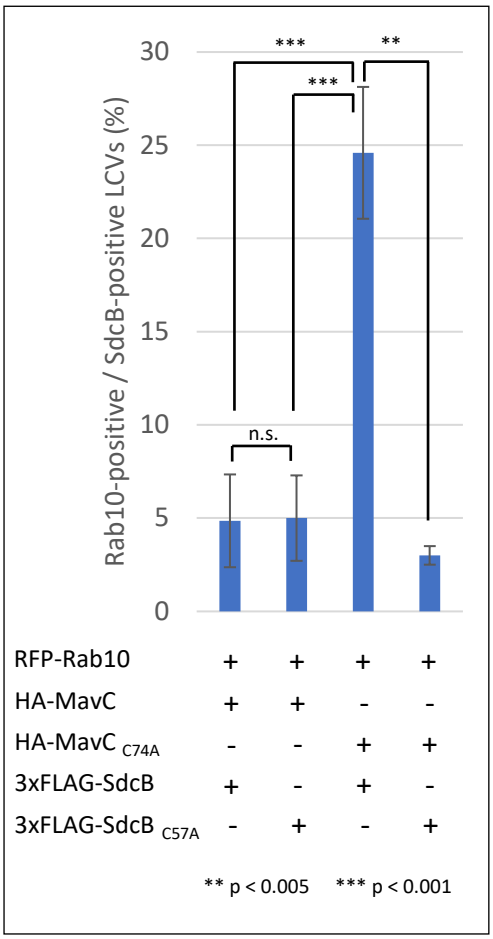
b
Rab10-positive / SdcB-positive LCVs (%)
30
25
20
15
10
5
0
***
***
**
n.s.
RFP-Rab10 + + + +
HA-MavC + + - -
HA-MavC C74A - - + +
3xFLAG-SdcB + - + -
3xFLAG-SdcB C57A - + - +
** p < 0.005 *** p < 0.001

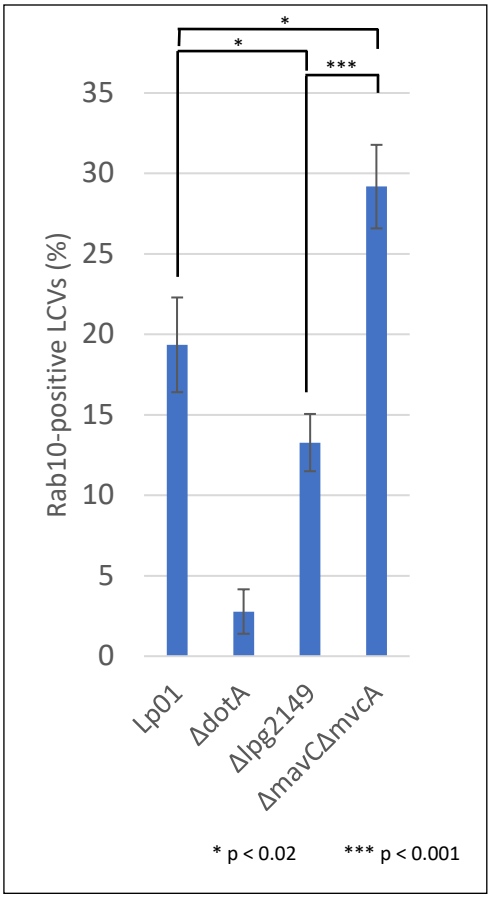
c
Rab10-positive LCVs (%)
35
30
25
20
15
10
5
0
*
*
***
Lp01
ΔdotA
Δlpg2149
ΔmavCΔmvcA
* p < 0.02 *** p < 0.001

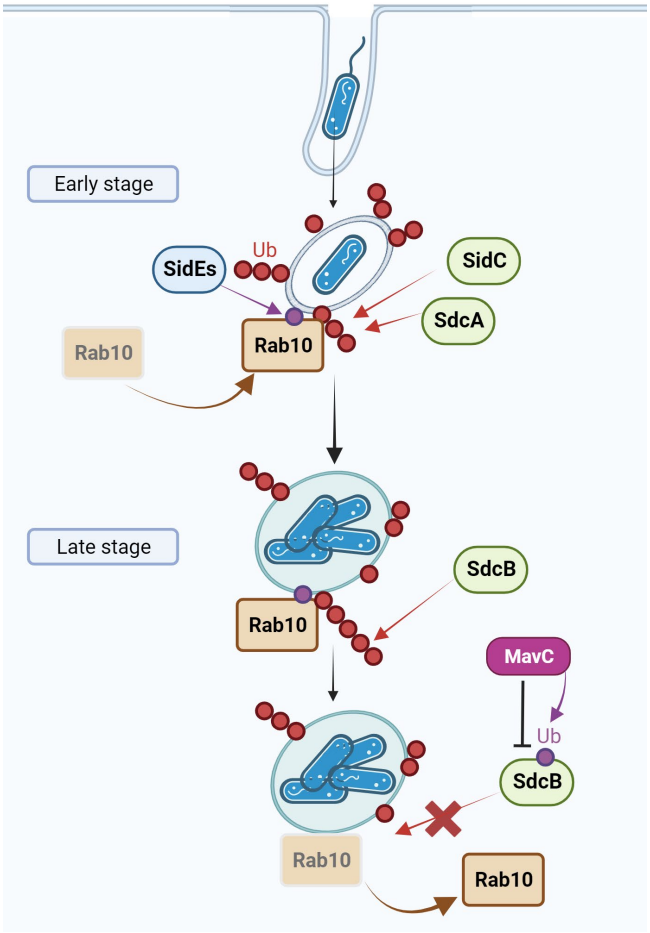
d
Early stage
SidEs
Ub
SidC
SdcA
Rab10
Rab10
Late stage
SdcB
Rab10
MavC
Ub
SdcB
Rab10
Rab10

Figure 7

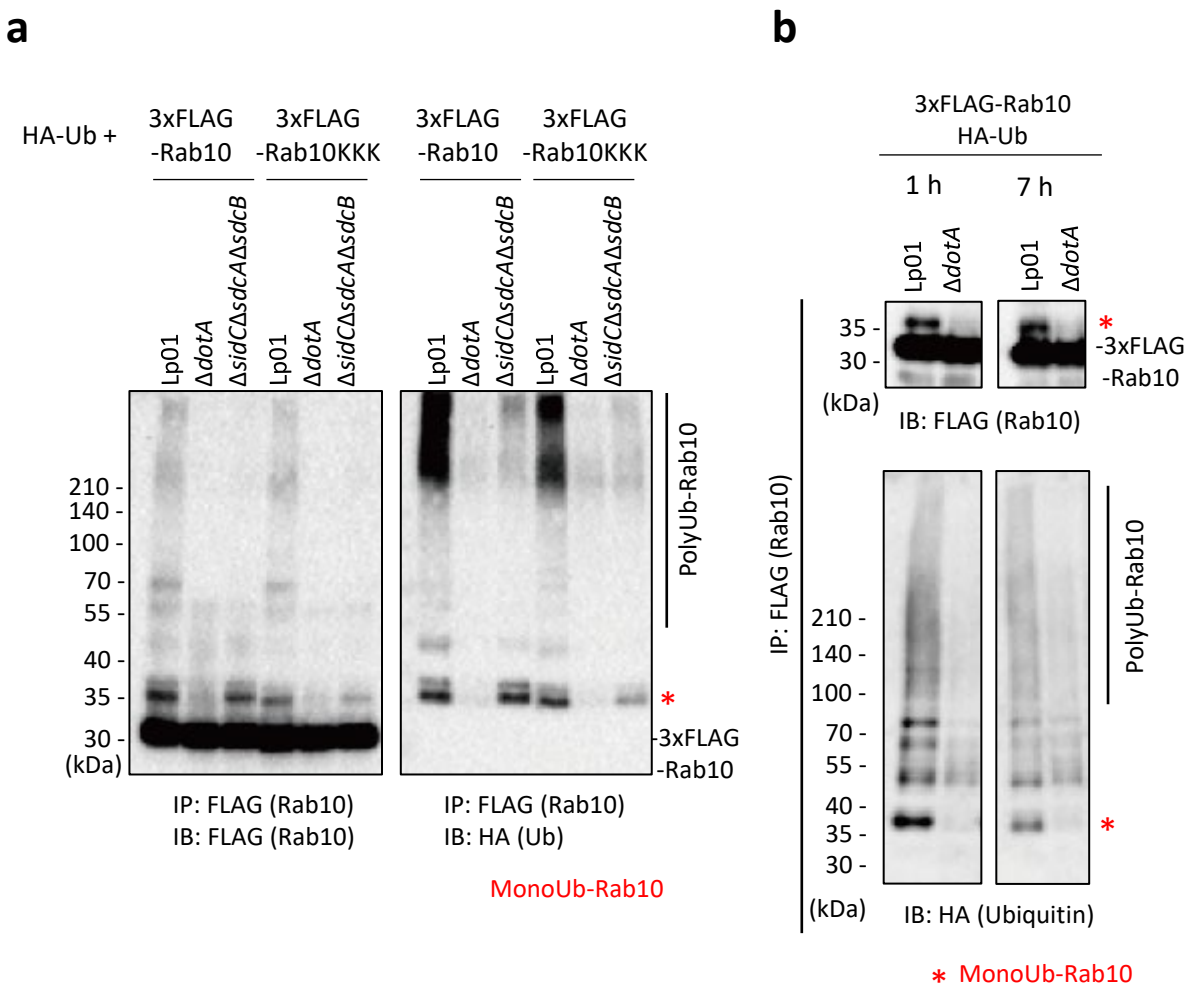

Figure 1 – figure supplement 1

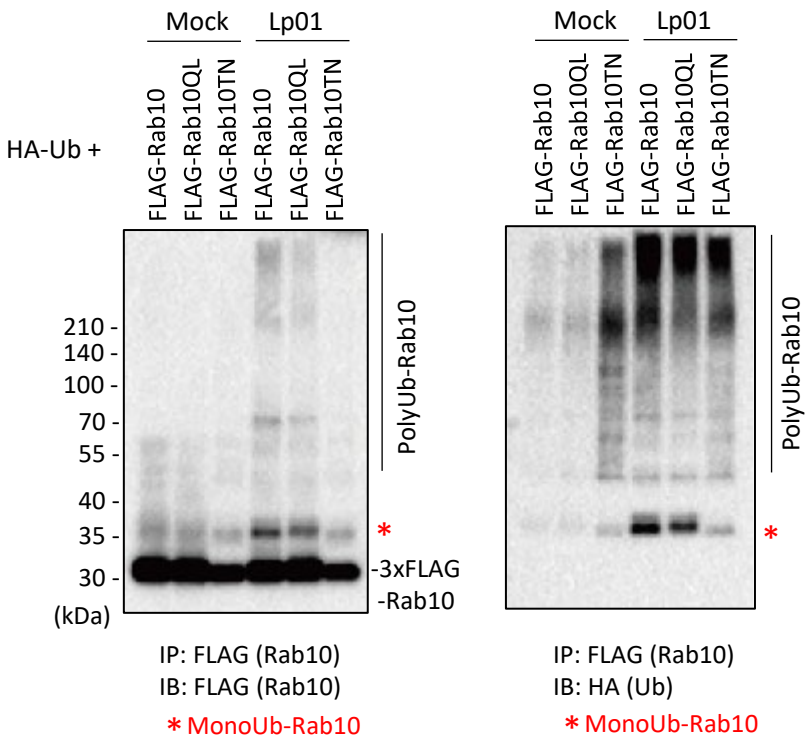

Figure 4 – figure supplement 1

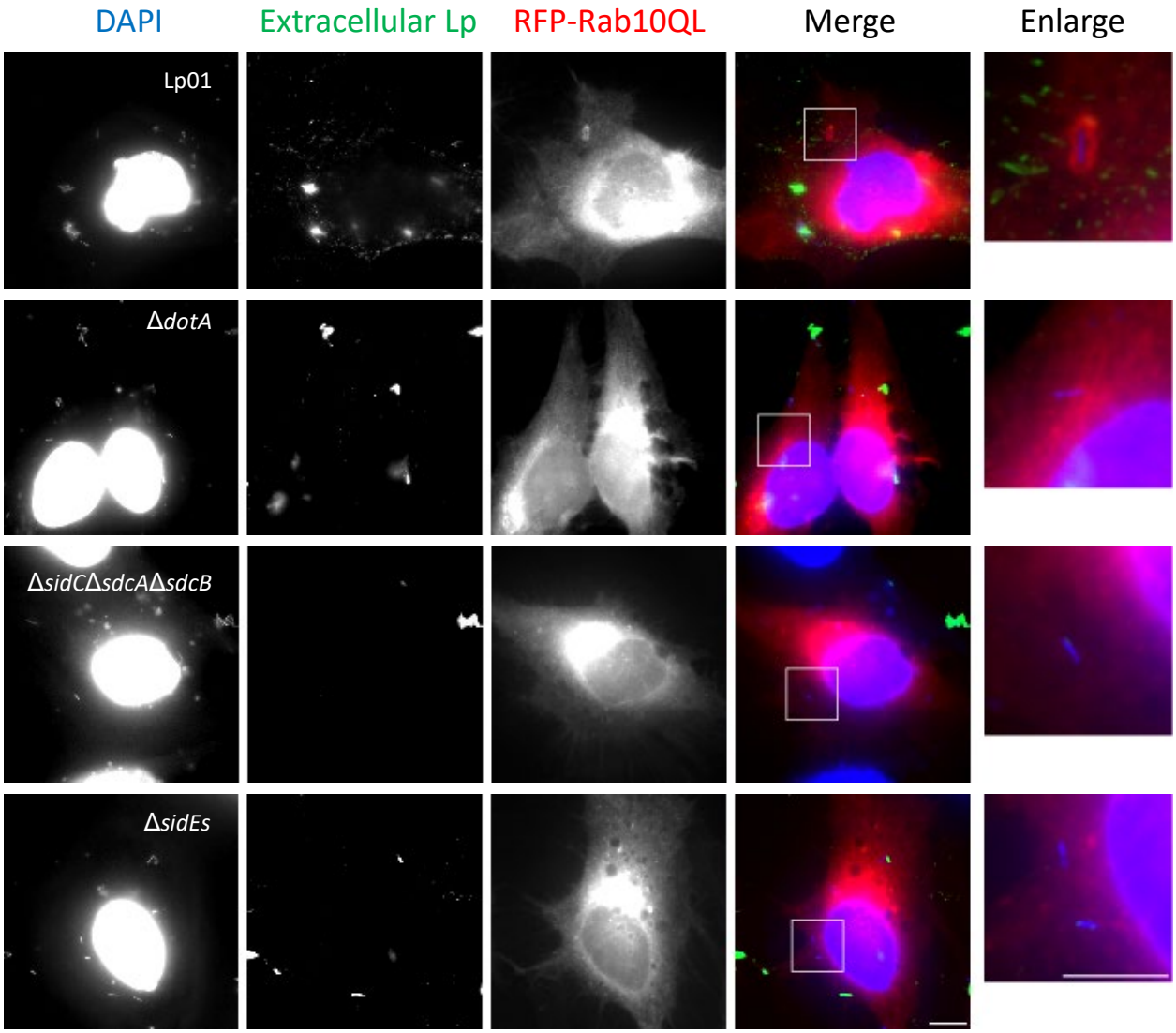

Figure 4 – figure supplement 2

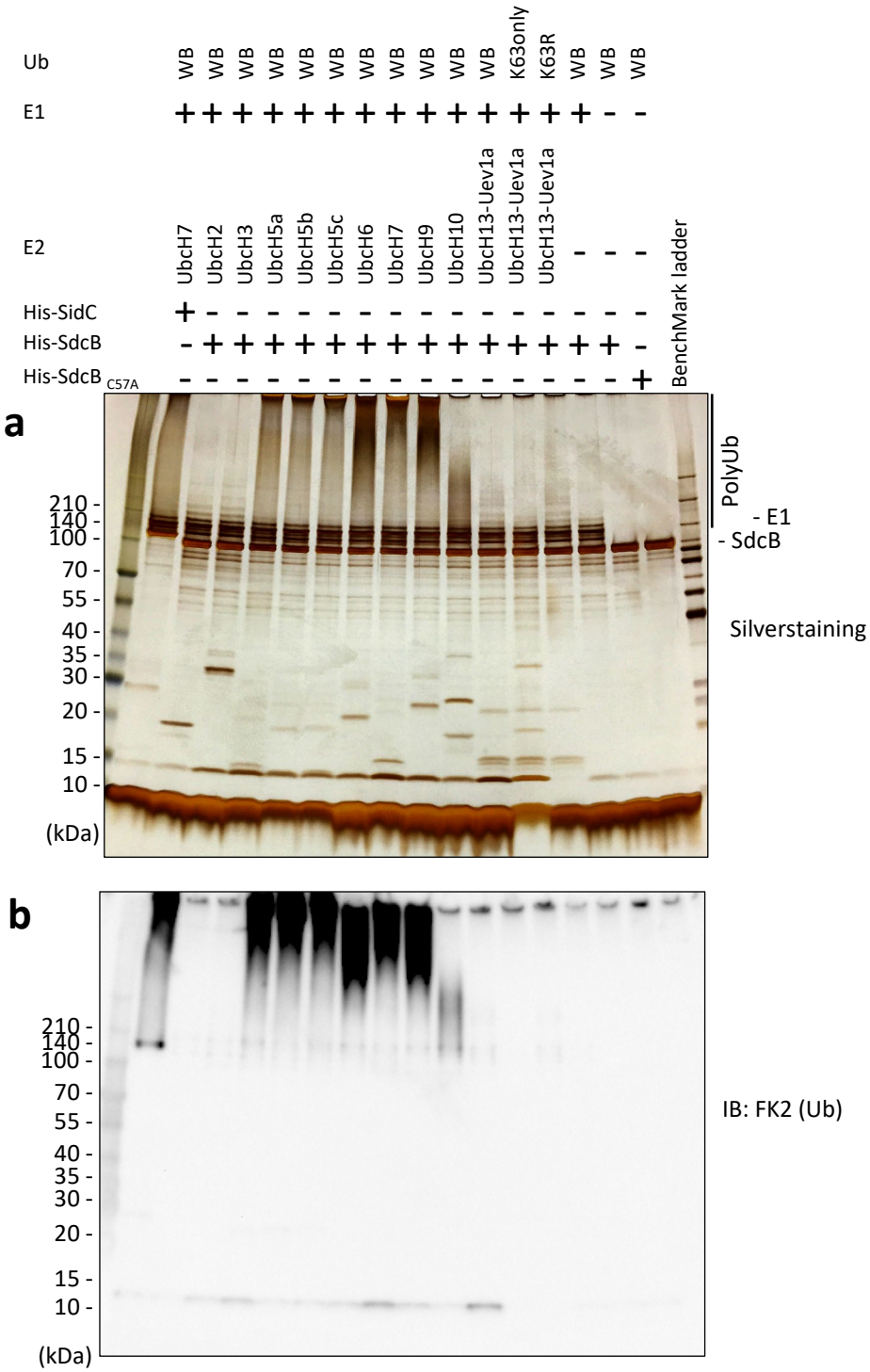

Figure 5 – figure supplement 1

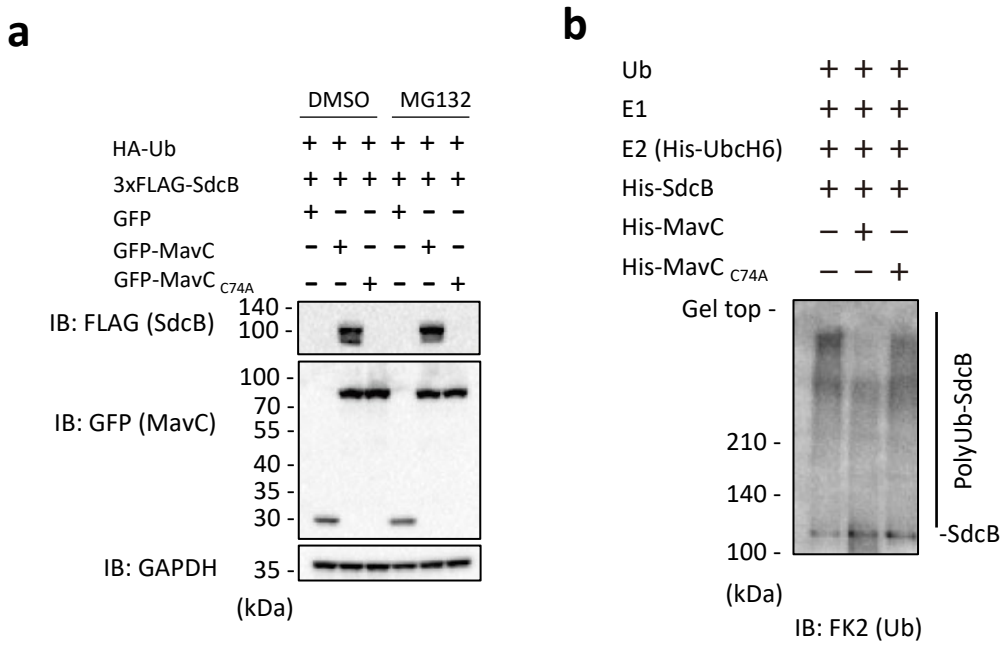

Figure 5 – figure supplement 2

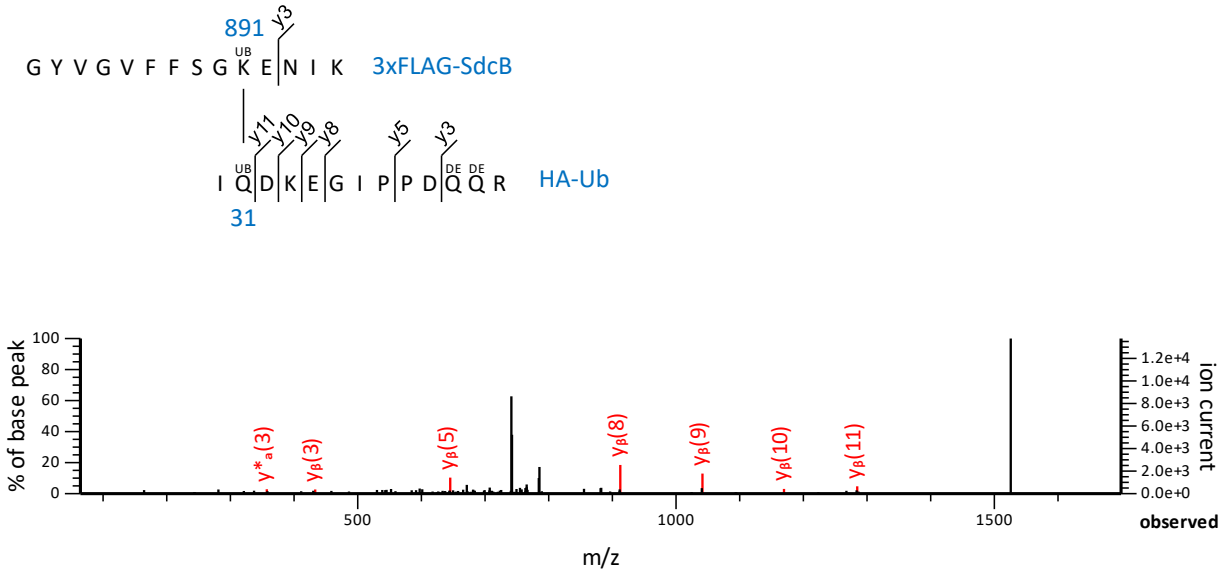

Figure 6 – figure supplement 1

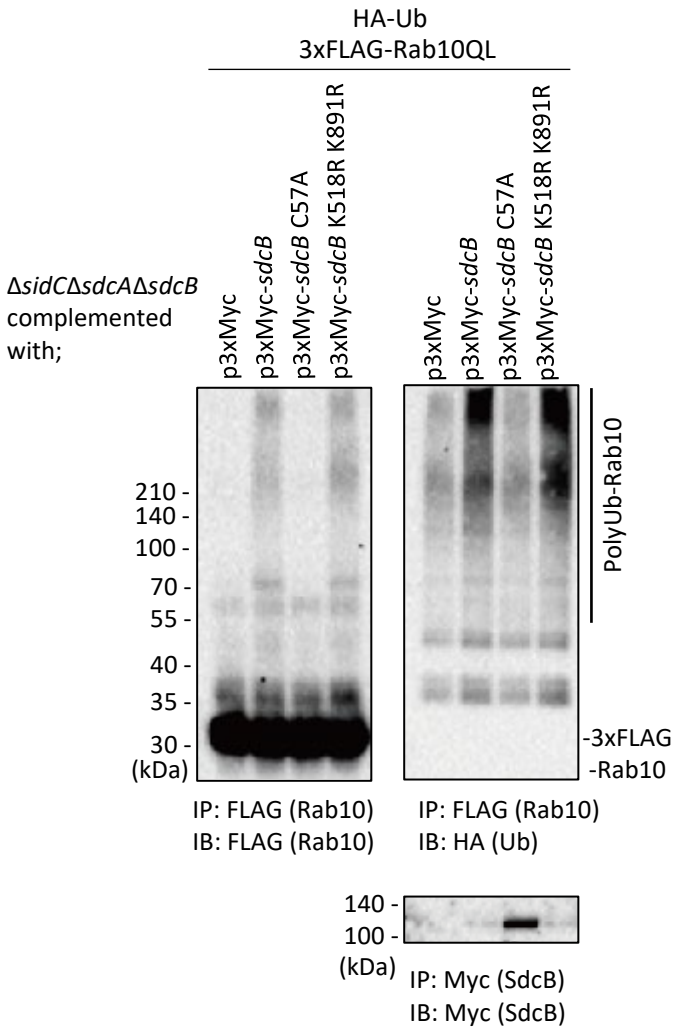

Figure 6 – figure supplement 2

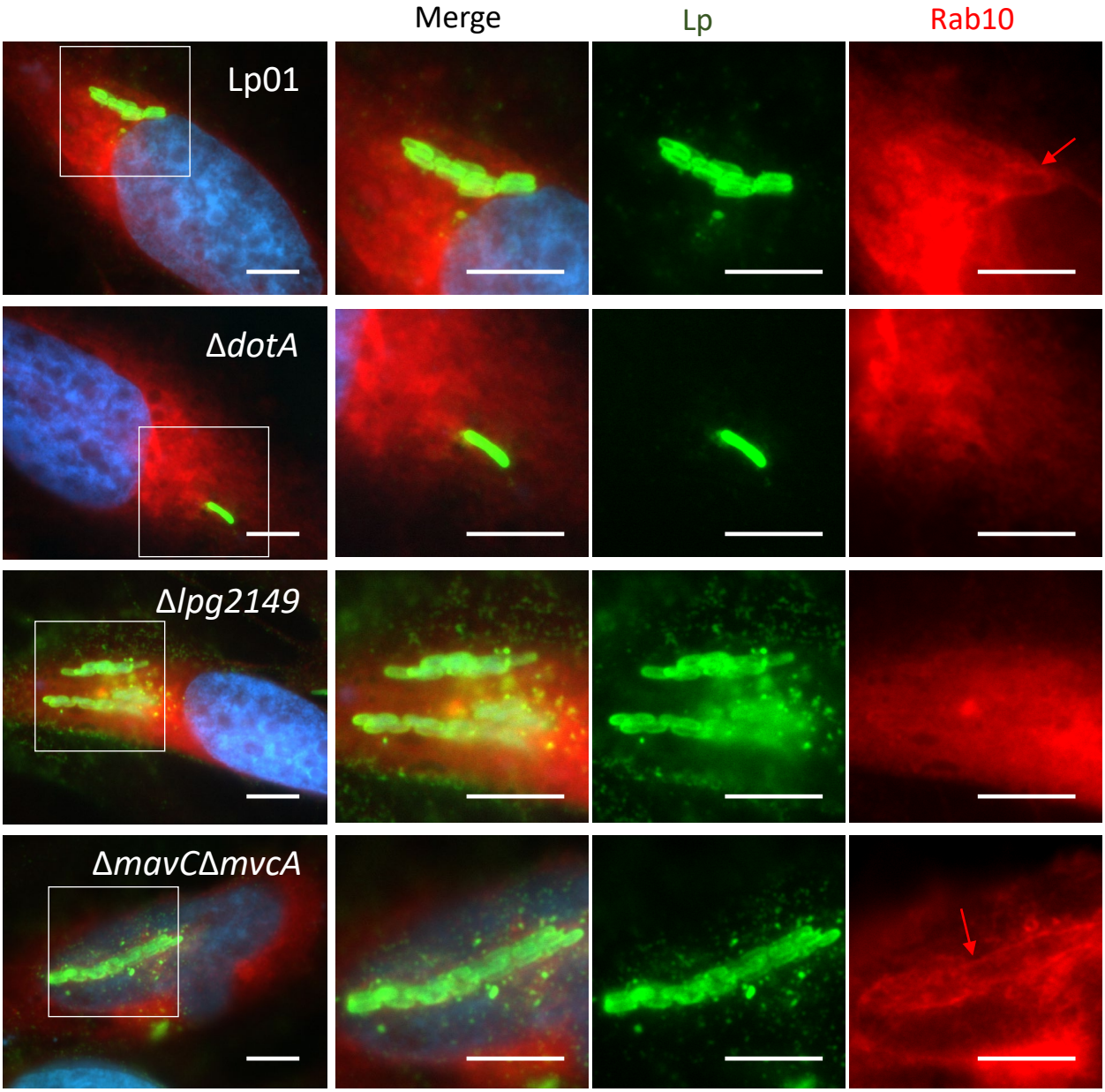

Figure 7 – figure supplement 1

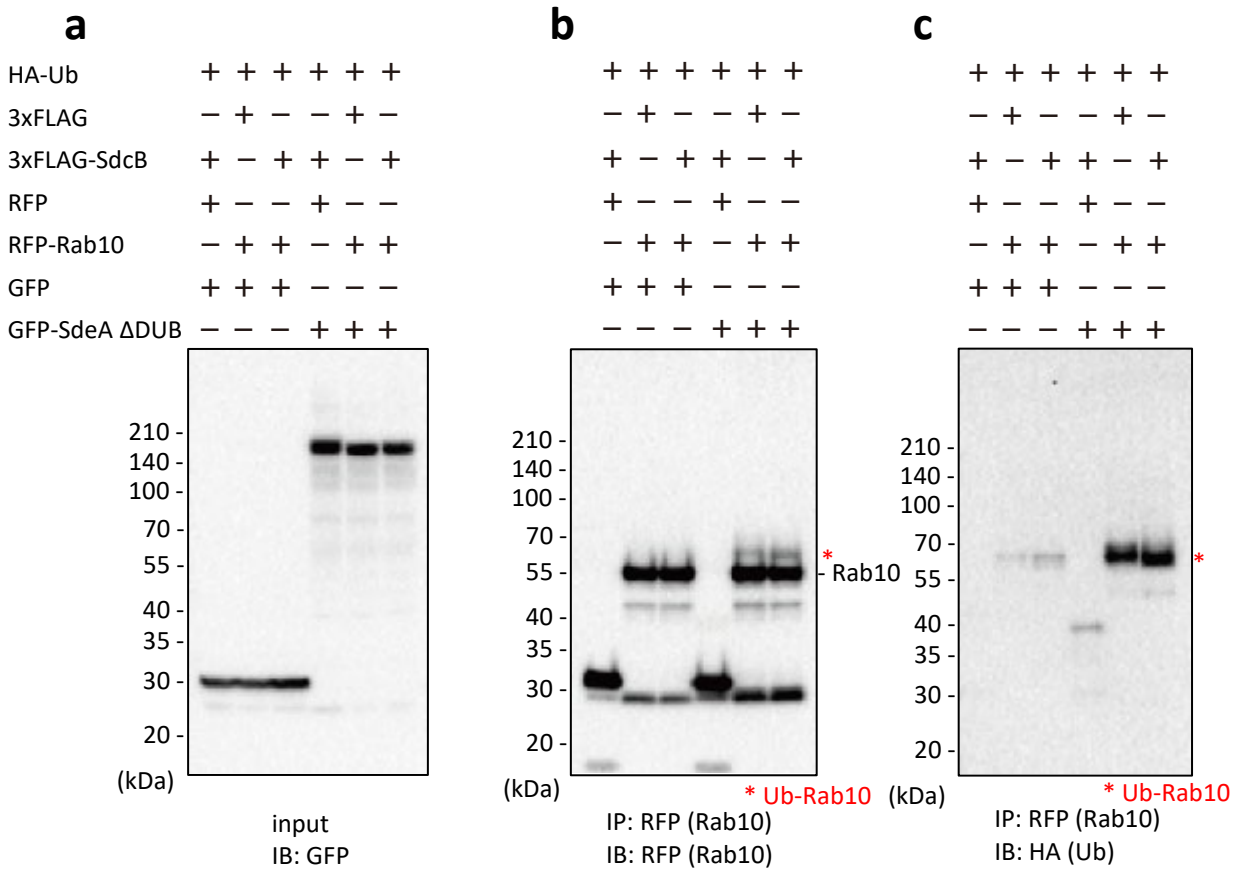

Figure 7 – figure supplement 2